Technische Universität Graz

Automated computation of topological derivatives with application to nonlinear elasticity and reaction-diffusion problems

P. Gangl, K. Sturm

**Berichte aus dem
Institut für Angewandte Mathematik**

Technische Universität Graz

Automated computation of topological derivatives with application to nonlinear elasticity and reaction-diffusion problems

P. Gangl, K. Sturm

**Berichte aus dem
Institut für Angewandte Mathematik**

Technische Universität Graz
Institut für Angewandte Mathematik
Steyrergasse 30
A 8010 Graz

WWW: `http://www.applied.math.tugraz.at`

AUTOMATED COMPUTATION OF TOPOLOGICAL DERIVATIVES WITH APPLICATION TO NONLINEAR ELASTICITY AND REACTION-DIFFUSION PROBLEMS

PETER GANGL AND KEVIN STURM

ABSTRACT.

Purpose While topological derivatives have proven useful in applications of topology optimisation and inverse problems, their mathematically rigorous derivation remains an ongoing research topic, in particular in the context of nonlinear partial differential equation (PDE) constraints.

Design/methodology/approach We present a systematic yet formal approach for the computation of topological derivatives of a large class of PDE-constrained topology optimization problems with respect to arbitrary inclusion shapes. Scalar and vector-valued as well as linear and nonlinear elliptic PDE constraints are considered in two and three space dimensions including a nonlinear elasticity model and nonlinear reaction-diffusion problems. The systematic procedure follows a Lagrangian approach for computing topological derivatives.

Findings For problems where the exact formula is known, the numerically computed values show good coincidence. Moreover, by inserting the computed values into the topological asymptotic expansion, we verify that the obtained values satisfy the expected behaviour also for other, previously unknown problems, indicating the correctness of the procedure.

Originality/value We present a systematic approach for the computation of topological derivatives that is applicable to a large class of problems. Most notably, our approach covers the topological derivative for a nonlinear elasticity problem, which has not been reported in the literature.

1. INTRODUCTION

The topological derivative concept was first used for finding optimal locations of holes in mechanical structures in [11] and was later introduced in a mathematically concise way in the publications [22] and [17]. Given a shape function $\mathcal{J}$ that maps a shape Ω to a real number $\mathcal{J}(\Omega)$, the topological derivative at a spatial point $z \in \Omega$ measures the sensitivity of $\mathcal{J}$ with respect to a small topological perturbation of the shape Ω. Denoting the perturbed shape by Ω_ε, e.g., $\Omega_\varepsilon := \Omega \setminus \omega_\varepsilon$ with $\omega_\varepsilon = B_\varepsilon(z)$, the topological derivative is defined as

$$d\mathcal{J}(\Omega)(z) := \lim_{\varepsilon \searrow 0} \frac{\mathcal{J}(\Omega_\varepsilon) - \mathcal{J}(\Omega)}{|\omega_\varepsilon|}, \tag{1.1}$$

thus satisfying a topologically asymptotic expansion of the form

$$\mathcal{J}(\Omega_\varepsilon) = \mathcal{J}(\Omega) + |\omega_\varepsilon| d\mathcal{J}(\Omega)(z) + o(\varepsilon) \quad \text{as } \varepsilon \searrow 0. \tag{1.2}$$

Since its introduction, the topological derivative concept has found application mostly in the context of topology optimization for engineering applications by level set approaches [4, 1, 9], but has also been utilized in medical applications such as electrical impedance tomography (EIT) [19] or mathematical image processing [18].

Most practically relevant engineering applications involve a partial differential equation (PDE) constraint and thus are of the type

$$\inf_\Omega J(\Omega, u) \qquad \text{subject to } e(\Omega; u) = 0 \tag{1.3}$$

with a PDE operator $e(\Omega; \cdot)$. In many cases (in particular when the principal part of the PDE operator is subject to a topological perturbation), the derivation of topological derivatives

involves an asymptotic analysis of the state variable of the form

$$u_\varepsilon(z + \varepsilon x) = u_0(z + \varepsilon x) + \varepsilon K(x) + o(\varepsilon) \quad \text{as } \varepsilon \searrow 0, \tag{1.4}$$

where u_ε is defined by the perturbed PDE operator, $e(\Omega_\varepsilon, u_\varepsilon) = 0$, and K is a corrector function defined as the solution to a transmission problem on the unbounded domain $\mathbf{R}^d$. Often, also a similar asymptotic analysis of an adjoint variable is needed. There exist different approaches for the derivation of topological derivatives for PDE-constrained optimization problems of the type (1.3). We mention the approaches by Novotny and Sokolowski [20], the approach by Amstutz [3] as well as the averaged adjoint approach [23]. Finally, we mention the approach that was introduced by Delfour in [10] and applied to quasilinear problems in [12, 14], which does not involve an asymptotic analysis of an adjoint variable.

For many problems involving linear or semilinear PDE constraints, topological derivatives are rather well-understood. In the cases where the shape of the inclusion ω is a disk or ellipse in 2D or a ball or ellipsoid in 3D, the corrector function K can be determined analytically and the topological derivative can be obtained in a closed form involving so-called polarisation tensors [2]. When ω has a more general shape as well as in the case of quasilinear PDE constraints, explicit formulas have not been reported in the literature. Topological derivatives in the context of quasilinear PDE constraints were first treated theoretically in [5], and later also in [12]. The numerical computation for a quasilinear problem was first discussed in [6] in the context of two-dimensional nonlinear magnetostatics, and later in the context of three-dimensional nonlinear magnetostatics in an $H(curl)$ setting in [14].

In this paper, we make the assumption that an expansion of the form (1.4) holds and apply the systematic approach of M.C. Delfour [10], see also [12], to a large class of problems involving linear and nonlinear elliptic PDEs as constraints. The suggested procedure covers scalar and vector-valued problems in two and three space dimensions. In particular, we will also treat the problem of nonlinear elasticity in two space dimensions using a St. Venant-Kirchhoff material which, to the best of the authors' knowledge, has not been reported on in the literature so far.

We stress that our generic automated approach is formal since a rigorous derivation would require a detailed asymptotic analysis of the variation of the state (1.4). Usually, this entails to show a sufficiently fast decay of the corrector K as $|x| \to \infty$. While the computation is formal, we show numerically that, for the considered problems, the computed values satisfy a topologically asymptotic expansion of the form (1.2).

2. Lagrangian approach for computing topological derivatives

In this section, we present the general approach for computing topological derivatives of a class of model problems based on the Lagrangian approach introduced in [10]. The considered problems include linear and nonlinear, scalar and vector-valued elliptic PDE constraints in two or three space dimensions.

2.1. Class of considered problems.
We consider a PDE-constrained shape optimization problem in d space dimensions where the solution to the PDE is $\mathbf{R}^m$-valued. This covers the case of scalar quantities, $m = 1$ or vector-valued problems such as elasticity, $m = d$. For a function $\varphi : \mathbf{R}^d \to \mathbf{R}^m$, we denote by $\mathcal{D}\varphi \in \mathbf{R}^{m \times d}$ its Jacobian, $(\mathcal{D}\varphi)_{i,k} = \frac{\partial \varphi_i}{\partial x_k}$ for $i \in \{1, \ldots m\}, k \in \{1, \ldots d\}$. We recall the Euclidean vector product $a \cdot b = \sum_{i=1}^m a_i b_i$ for $a, b \in \mathbf{R}^m$ and will also use this notation for $m = 1$, noting that the vector product is just a simple product then. Moreover, we denote by $A : B = \sum_{i=1}^m \sum_{k=1}^d A_{i,k} B_{i,k}$ the Frobenius inner product of two matrices $A, B \in \mathbf{R}^{m \times d}$ and again note that the Frobenius inner product reduces to the Euclidean inner product of two vectors when $m = 1$.

We consider a computational domain D which is subdivided into two open disjoint subdomains, $\mathsf{D} = \Omega^{\text{in}} \cup \Omega^{\text{out}}$. We introduce the abbreviation $\Omega := \Omega^{\text{in}}$, such that $\Omega^{\text{out}} = \mathsf{D} \setminus \overline{\Omega}$.

Moreover, we consider four operators

$$A_1^{\mathrm{in}}, A_1^{\mathrm{out}} : \mathsf{D} \times \mathbf{R}^m \times \mathbf{R}^{m \times d} \to \mathbf{R}^m$$
$$A_2^{\mathrm{in}}, A_2^{\mathrm{out}} : \mathsf{D} \times \mathbf{R}^m \times \mathbf{R}^{m \times d} \to \mathbf{R}^{m \times d}$$

to define the two piecewise defined operators $A_1^\Omega : \mathsf{D} \times \mathbf{R}^m \times \mathbf{R}^{m \times d} \to \mathbf{R}^m$, $A_2^\Omega : \mathsf{D} \times \mathbf{R}^m \times \mathbf{R}^{m \times d} \to \mathbf{R}^{m \times d}$,

$$A_1^\Omega(x, y_1, y_2) := \chi_\Omega(x) A_1^{\mathrm{in}}(x, y_1, y_2) + \chi_{\mathsf{D} \setminus \Omega}(x) A_1^{\mathrm{out}}(x, y_1, y_2), \tag{2.1}$$

$$A_2^\Omega(x, y_1, y_2) := \chi_\Omega(x) A_2^{\mathrm{in}}(x, y_1, y_2) + \chi_{\mathsf{D} \setminus \Omega}(x) A_2^{\mathrm{out}}(x, y_1, y_2), \tag{2.2}$$

which will represent the left hand side of an abstract PDE constraint. The right hand side will comprise $F_1^\Omega : \mathsf{D} \to \mathbf{R}^m$, $F_2^\Omega : \mathsf{D} \to \mathbf{R}^{m \times d}$ with

$$F_i^\Omega(x) := \chi_\Omega(x) F_i^{\mathrm{in}}(x) + \chi_{\mathsf{D} \setminus \Omega}(x) F_i^{\mathrm{out}}(x), \tag{2.3}$$

for $i = 1, 2$ with functions $F_1^{\mathrm{in}}, F_1^{\mathrm{out}} : \mathsf{D} \to \mathbf{R}^m$ and $F_2^{\mathrm{in}}, F_2^{\mathrm{out}} : \mathsf{D} \to \mathbf{R}^{m \times d}$. Finally, we assume that the boundary $\partial \mathsf{D}$ of D is subdivided into two subsets Γ_D, Γ_N and consider a function $g_N : \Gamma_N \to \mathbf{R}^m$ to represent inhomogeneous Neumann boundary conditions. For sake of more compact presentation, we only consider homogeneous Dirichlet conditions on the Dirichlet boundary Γ_D and remark that an extension to inhomogenous conditions can be obtained by minor modifications. For a given admissible subdomain $\Omega \subset \mathsf{D}$, we consider the PDE constraint to find $u \in \mathbf{E}(\mathsf{D})$ such that

$$\int_\mathsf{D} A_1^\Omega(x, u, \mathcal{D}u) \cdot \psi + A_2^\Omega(x, u, \mathcal{D}u) : \mathcal{D}\psi \, \mathrm{d}x = \int_\mathsf{D} F_1^\Omega(x) \cdot \psi + F_2^\Omega(x) : \mathcal{D}\psi \, \mathrm{d}x + \int_{\Gamma_N} g_N \cdot \psi \, \mathrm{d}S \tag{2.4}$$

for all $\psi \in \mathbf{E}(\mathsf{D})$, where $\mathbf{E}(\mathsf{D})$ is the function space on which the PDE is posed and which includes the homogeneous Dirichlet conditions on Γ_D. Similarly, we consider two functions $j^{\mathrm{in}}, j^{\mathrm{out}} : \mathsf{D} \times \mathbf{R}^m \times \mathbf{R}^{m \times d} \to \mathbf{R}$ and, for a given admissible set $\Omega \subset \mathsf{D}$, define the piecewise defined function $j^\Omega : \mathsf{D} \times \mathbf{R}^m \times \mathbf{R}^{m \times d} \to \mathbf{R}$,

$$j^\Omega(x, y_1, y_2) := \chi_\Omega(x) j^{\mathrm{in}}(x, y_1, y_2) + \chi_{\mathsf{D} \setminus \Omega}(x) j^{\mathrm{out}}(x, y_1, y_2). \tag{2.5}$$

For $\varphi \in \mathbf{E}(\mathsf{D})$, we will consider the cost function

$$J(\Omega, \varphi, \mathcal{D}\varphi) := J^{\mathrm{vol}}(\Omega, \varphi, \mathcal{D}\varphi) + J^{\mathrm{bnd}}(\varphi, \mathcal{D}\varphi) \tag{2.6}$$

with

$$J^{\mathrm{vol}}(\Omega, \varphi, \mathcal{D}\varphi) := \int_\mathsf{D} j^\Omega(x, \varphi, \mathcal{D}\varphi) \, dx, \qquad J^{\mathrm{bnd}}(\varphi, \mathcal{D}\varphi) := \int_{\partial \mathsf{D}} j^{bnd}(x, \varphi, \mathcal{D}\varphi) \, dS \tag{2.7}$$

for a function $j^{bnd} : \partial \mathsf{D} \times \mathbf{R}^m \times \mathbf{R}^{m \times d} \to \mathbf{R}$. Summarizing, we consider the abstract class of PDE-constrained topology optimization problem which can be written as

$$\begin{aligned} &\min_{\Omega \in \mathcal{A}} J^{\mathrm{vol}}(\Omega, u, \mathcal{D}u) + J^{\mathrm{bnd}}(u, \mathcal{D}u) \\ &\text{subject to } u \in \mathbf{E}(\mathsf{D}) \text{ solves (2.4)} \end{aligned} \tag{2.8}$$

where $\mathcal{A}$ denotes the set of admissible subsets of D.

Remark 1. *Although we consider only homogeneous boundary conditions, the formulas for inhomogeneous Dirichlet boundary conditions will not affect the formula of the first topological derivative; see, e.g., [8] where mixed (Dirichlet and Neumann) inhomogeneous boundary conditions are considered.*

2.2. **Domain perturbation.** Let $\omega \subset \mathbf{R}^d$ with $0 \in \omega$ represent the shape of the considered topological perturbation. For a point $z \in \mathsf{D} \setminus \partial\Omega$ and a given small parameter ε, we define $\omega_\varepsilon(z) := z + \varepsilon\omega$ as well as the perturbed domain

$$\Omega_\varepsilon(z) := \begin{cases} \Omega \setminus \overline{\omega}_\varepsilon(z), & z \in \Omega, \\ \Omega \cup \omega_\varepsilon(z), & z \in \mathsf{D} \setminus \overline{\Omega}. \end{cases}$$

From now on, we assume that a fixed point $z \in \mathsf{D} \setminus \overline{\Omega}$ is given and set $\omega_\varepsilon := \omega_\varepsilon(z)$, $\Omega_\varepsilon := \Omega_\varepsilon(z)$. Moreover, we use the abbreviation $\mathsf{D}_\varepsilon := T_\varepsilon^{-1}(\mathsf{D})$, where $T_\varepsilon(x) := z + \varepsilon x$. We also introduce the abbreviating notations $A_1^{(\varepsilon)} := A_1^{\Omega_\varepsilon}$, $A_2^{(\varepsilon)} := A_2^{\Omega_\varepsilon}$, $F_1^{(\varepsilon)} := F_1^{\Omega_\varepsilon}$, $F_2^{(\varepsilon)} := F_2^{\Omega_\varepsilon}$, $j^{(\varepsilon)} := j^{\Omega_\varepsilon}$ and define the perturbed Lagrangian of the abstract optimization problem (2.8)

$$G(\varepsilon, \varphi, \mathcal{D}\varphi, \psi, \mathcal{D}\psi) = J(\Omega_\varepsilon, \varphi, \mathcal{D}\varphi) + \langle A_1^{(\varepsilon)}(\varphi, \mathcal{D}\varphi), \psi \rangle + \langle A_2^{(\varepsilon)}(\varphi, \mathcal{D}\varphi), \mathcal{D}\psi \rangle$$
$$- \langle F_1^{(\varepsilon)}, \psi \rangle - \langle F_2^{(\varepsilon)}, \mathcal{D}\psi \rangle - \langle g_N, \psi \rangle,$$

where $\langle \cdot, \cdot \rangle$ denotes the duality product in the corresponding spaces.

2.3. **Formal variation of the state variable.** The following derivation is motivated by the rigorous results obtained in [12], where a simplified approach to the computation of quasi-linear derivatives is proposed. Here we generalise these results formally to the class of non-linear problems introduced in (2.8). We also refer to [6, 5] for another approach to the computation of topological derivatives for quasi-linear problems.

Let $\psi \in \mathbf{E}(\mathsf{D})$. The perturbed state equation reads: u_ε solves

$$\int_{\mathsf{D}} A_1^{(\varepsilon)}(x, u_\varepsilon, \mathcal{D}u_\varepsilon) \cdot \psi + A_2^{(\varepsilon)}(x, u_\varepsilon, \mathcal{D}u_\varepsilon) : \mathcal{D}\psi \, dx = \int_{\mathsf{D}} F_1^{(\varepsilon)}(x) \cdot \psi + F_2^{(\varepsilon)}(x) : \mathcal{D}\psi \, dx$$
$$+ \int_{\Gamma_N} g_N \cdot \psi \, dS. \tag{2.9}$$

Subtracting the state equation (2.9) for $\varepsilon > 0$ from the state equation for $\varepsilon = 0$ leads to

$$\int_{\mathsf{D}} [A_1^{(\varepsilon)}(x, u_\varepsilon, \mathcal{D}u_\varepsilon) - A_1^{(0)}(x, u_0, \mathcal{D}u_0)] \cdot \psi + [A_2^{(\varepsilon)}(x, u_\varepsilon, \mathcal{D}u_\varepsilon) - A_2^{(0)}(x, u_0, \mathcal{D}u_0)] : \mathcal{D}\psi \, dx$$
$$= \int_{\omega_\varepsilon} (F_1^{\mathrm{in}} - F_1^{\mathrm{out}})(x) \cdot \psi + (F_2^{\mathrm{in}} - F_2^{\mathrm{out}})(x) : \mathcal{D}\psi \, dx.$$

Using the change of variables $T_\varepsilon(x) = z + \varepsilon x$, we obtain with the notation $\mathsf{D}_\varepsilon = T_\varepsilon^{-1}(\mathsf{D})$:

$$\int_{\mathsf{D}_\varepsilon} [A_1^{(\varepsilon)}(T_\varepsilon(x), u_\varepsilon \circ T_\varepsilon, (\mathcal{D}u_\varepsilon) \circ T_\varepsilon) - A_1^{(0)}(T_\varepsilon(x), u_0 \circ T_\varepsilon, (\mathcal{D}u_0) \circ T_\varepsilon)] \cdot (\psi \circ T_\varepsilon)$$
$$+ [A_2^{(\varepsilon)}(T_\varepsilon(x), u_\varepsilon \circ T_\varepsilon, (\mathcal{D}u_\varepsilon) \circ T_\varepsilon) - A_2^{(0)}(T_\varepsilon(x), u_0 \circ T_\varepsilon, (\mathcal{D}u_0) \circ T_\varepsilon)] : (\mathcal{D}\psi) \circ T_\varepsilon \, dx$$
$$= \int_\omega ((F_1^{\mathrm{in}} - F_1^{\mathrm{out}}) \circ T_\varepsilon) \cdot (\psi \circ T_\varepsilon) + ((F_2^{\mathrm{in}} - F_2^{\mathrm{out}}) \circ T_\varepsilon) : ((\mathcal{D}\psi) \circ T_\varepsilon) \, dx.$$

Using $(\mathcal{D}\varphi) \circ T_\varepsilon = \frac{1}{\varepsilon}\mathcal{D}(\varphi \circ T_\varepsilon)$ and the first variation of the state $K_\varepsilon := \frac{(u_\varepsilon - u_0) \circ T_\varepsilon}{\varepsilon}$, after multiplication with ε, we obtain

$$\int_{\mathsf{D}_\varepsilon} [A_1^{(\varepsilon)}(T_\varepsilon(x), u_0 \circ T_\varepsilon + \varepsilon K_\varepsilon, (\mathcal{D}u_0) \circ T_\varepsilon + \mathcal{D}K_\varepsilon)$$
$$- A_1^{(0)}(T_\varepsilon(x), u_0 \circ T_\varepsilon, (\mathcal{D}u_0) \circ T_\varepsilon)] \cdot (\varepsilon\psi \circ T_\varepsilon)$$
$$+ \int_{\mathsf{D}_\varepsilon} [A_2^{(\varepsilon)}(T_\varepsilon(x), u_0 \circ T_\varepsilon + \varepsilon K_\varepsilon, (\mathcal{D}u_0) \circ T_\varepsilon + \mathcal{D}K_\varepsilon)$$
$$- A_2^{(0)}(T_\varepsilon(x), u_0 \circ T_\varepsilon, (\mathcal{D}u_0) \circ T_\varepsilon)] : \mathcal{D}(\psi \circ T_\varepsilon) \, dx$$
$$= \int_\omega ((F_1^{\mathrm{in}} - F_1^{\mathrm{out}}) \circ T_\varepsilon) \cdot (\varepsilon\psi \circ T_\varepsilon) + ((F_2^{\mathrm{in}} - F_2^{\mathrm{out}}) \circ T_\varepsilon) : \mathcal{D}(\psi \circ T_\varepsilon) \, dx.$$

Now we make the following assumption:

Assumption 1. (i) *We assume that u_0 is continuously differentiable at z.*

(ii) *Let $K_\varepsilon := \frac{(u_\varepsilon - u_0)\circ T_\varepsilon}{\varepsilon}$ for $\varepsilon > 0$ be the first variation of the state variable u_ε. We assume that $\nabla K_\varepsilon \to \nabla K$ and $\varepsilon K_\varepsilon \to 0$, where K solves (2.11).*

(iii) *For all $\varepsilon > 0$ we have $\psi \in \mathbf{E}(\mathsf{D}_\varepsilon)$ if and only if $\psi \circ T_\varepsilon \in \mathbf{E}(\mathsf{D})$.*

Rearranging and replacing $\psi \circ T_\varepsilon$ by ψ (using Assumption 1,item (iii)) yields

$$
\begin{aligned}
&\int_{\mathsf{D}_\varepsilon} [A_1^{(\varepsilon)}(T_\varepsilon(x), u_0 \circ T_\varepsilon + \varepsilon K_\varepsilon, (\mathcal{D}u_0)\circ T_\varepsilon + \mathcal{D}K_\varepsilon) - A_1^{(\varepsilon)}(T_\varepsilon(x), u_0 \circ T_\varepsilon, (\mathcal{D}u_0)\circ T_\varepsilon)]\cdot \varepsilon\psi \\
&\quad + [A_2^{(\varepsilon)}(T_\varepsilon(x), u_0 \circ T_\varepsilon + \varepsilon K_\varepsilon, (\mathcal{D}u_0)\circ T_\varepsilon + \mathcal{D}K_\varepsilon) - A_2^{(\varepsilon)}(T_\varepsilon(x), u_0 \circ T_\varepsilon, (\mathcal{D}u_0)\circ T_\varepsilon)] : \mathcal{D}\psi \, dx \\
&= \int_\omega ((F_1^{\mathrm{in}} - F_1^{\mathrm{out}})\circ T_\varepsilon)\cdot(\varepsilon\psi) + ((F_2^{\mathrm{in}} - F_2^{\mathrm{out}})\circ T_\varepsilon) : \mathcal{D}\psi \, dx \\
&\quad - \int_\omega [A_1^{\mathrm{in}} - A_1^{\mathrm{out}}](T_\varepsilon(x), u_0 \circ T_\varepsilon, (\mathcal{D}u_0)\circ T_\varepsilon)\cdot\varepsilon\psi \, dx \\
&\quad - \int_\omega [A_2^{\mathrm{in}} - A_2^{\mathrm{out}}](T_\varepsilon(x), u_0 \circ T_\varepsilon, (\mathcal{D}u_0)\circ T_\varepsilon) : \mathcal{D}\psi \, dx
\end{aligned}
\tag{2.10}
$$

for all $\psi \in \mathbf{E}(\mathsf{D}_\varepsilon)$. With this we can pass to limit $\varepsilon \to 0$ in (2.10) and get

$$
\begin{aligned}
&\int_{\mathbf{R}^d} [A_2^\omega(z, u_0(z), \mathcal{D}u_0(z) + \mathcal{D}K) - A_2^\omega(z, u_0(z), \mathcal{D}u_0(z))] : \mathcal{D}\psi \, dx \\
&\quad = \int_\omega (F_2^{\mathrm{in}} - F_2^{\mathrm{out}})(z) : \mathcal{D}\psi \, dx - \int_\omega [A_2^{\mathrm{in}} - A_2^{\mathrm{out}}](z, u_0(z), \mathcal{D}u_0(z)) : \mathcal{D}\psi \, dx,
\end{aligned}
\tag{2.11}
$$

for all $\psi \in \mathbf{E}(\mathbf{R}^d) := \lim_{\varepsilon \searrow 0} \mathbf{E}(\mathsf{D}_\varepsilon)$, with the definition $A_2^\omega(x, y_1, y_2) = \chi_\omega(x)A_2^{\mathrm{in}}(x, y_1, y_2) + \chi_{\mathbf{R}^d \setminus \omega}(x)A_2^{\mathrm{out}}(x, y_1, y_2)$. The limit $\lim_{\varepsilon \searrow 0} \mathbf{E}(\mathsf{D}_\varepsilon)$ has to be understood formally and in practice often is a Beppo-Levi space (see the next remark).

Remark 2. *The function space $\mathbf{E}(\mathbf{R}^d)$ in which (2.11) admits a solution can often be chosen as a Beppo-Levi space as shown in [23], see also [12]. For the numerical approximation in the next section we use precisely that the functions K_ε converge to K and approximate K by solving an equation on a blown up domain similarly to D_ε.*

2.4. **Lagrangian theorem for first topological derivatives.** In this section we discuss a method proposed by M.C. Delfour in [10, Thm.3.3]. The definite advantage is that it uses the unperturbed adjoint equation and only requires the asymptotic analysis of the state equation, but it seems to come with the shortcoming that certain cost functions cannot be treated rigorously; see [12] and also [8].

Let $\mathbf{E}(\mathsf{D})$ be a Banach space of functions on D. For all parameter $\varepsilon \geq 0$ small consider a function $u_\varepsilon \in \mathbf{E}(\mathsf{D})$ solving the variational problem of the form

$$
a_\varepsilon[u_\varepsilon](\varphi) = f_\varepsilon(\varphi) \quad \text{for all } \varphi \in \mathbf{E}(\mathsf{D}),
\tag{2.12}
$$

where $a_\varepsilon : \mathbf{E}(\mathsf{D}) \to \mathbf{E}(\mathsf{D})'$ is a nonlinear operator and f_ε is a linear form on $\mathbf{E}(\mathsf{D})$, respectively. Throughout we assume that this abstract state equation admits a unique solution and that $u_\varepsilon - u_0 \in \mathbf{E}(\mathsf{D})$ for all ε. Consider now a cost function

$$
j(\varepsilon) = J_\varepsilon(u_\varepsilon) \in \mathbf{R},
\tag{2.13}
$$

where for all $\varepsilon \geq 0$ the functional $J_\varepsilon : \mathbf{E}(\mathsf{D}) \to \mathbf{R}$ is differentiable at u_0. In the following sections we review methods how to obtain an asymptotic expansion of $j(\varepsilon)$ at $\varepsilon = 0$. For this purpose we introduce the Lagrangian function

$$
\mathfrak{L}(\varepsilon, u, v) = J_\varepsilon(u) + a_\varepsilon[u](v) - f_\varepsilon(v), \quad u \in \mathbf{E}(\mathsf{D}), \; v \in \mathbf{E}(\mathsf{D}).
$$

Proposition 1 ([10])**.** *Let $\ell : [0, \tau] \to \mathbf{R}$ be a function with $\ell(\varepsilon) > 0$ for $\varepsilon > 0$ and $\lim\limits_{\varepsilon \searrow 0} \ell(\varepsilon) = 0$. Furthermore, assume that the limits*

$$\mathfrak{R}_1(u_0, p_0) := \lim_{\varepsilon \searrow 0} \frac{1}{\ell(\varepsilon)} \int_0^1 [\partial_u \mathfrak{L}(\varepsilon, s u_\varepsilon + (1-s) u_0, p_0) - \partial_u \mathfrak{L}(\varepsilon, u_0, p_0)(u_\varepsilon - u_0)] \, ds, \quad (2.14)$$

$$\mathfrak{R}_2(u_0, p_0) := \lim_{\varepsilon \searrow 0} \frac{1}{\ell(\varepsilon)} (\partial_u \mathfrak{L}(\varepsilon, u_0, p_0) - \partial_u \mathfrak{L}(0, u_0, p_0))(u_\varepsilon - u_0), \quad (2.15)$$

$$\partial_\ell \mathfrak{L}(0, u_0, p_0) := \lim_{\varepsilon \searrow 0} \frac{1}{\ell(\varepsilon)} (\mathfrak{L}(\varepsilon, u_0, p_0) - \mathfrak{L}(0, u_0, p_0)), \quad (2.16)$$

exist. Then the following expansion holds:

$$j(\varepsilon) = j(0) + \ell(\varepsilon)((\mathfrak{R}_1(u_0, p_0) + \mathfrak{R}_2(u_0, p_0) + \partial_\ell \mathfrak{L}(0, u_0, p_0)) + o(\ell(\varepsilon)). \quad (2.17)$$

Remark 3. *Note that by the fundamental theorem of calculus $\mathfrak{R}_1$ can be equivalently written as*

$$\mathfrak{R}_1(u_0, p_0) = \lim_{\varepsilon \searrow 0} \frac{1}{\ell(\varepsilon)} [\mathfrak{L}(\varepsilon, u_\varepsilon, p_0) - \mathfrak{L}(\varepsilon, u_0, p_0) - \partial_u \mathfrak{L}(\varepsilon, u_0, p_0)(u_\varepsilon - u_0)].$$

However, the form stated in the proposition is better suited for the formal computation of the topological derivatives presented later on.

2.5. **Formal computation of topological derivative.** We are now applying formally Proposition 1 to compute the topological derivative of problem (2.8). For this we let $\mathfrak{L}(\varepsilon, \varphi, \psi) := G(\varepsilon, \varphi, \mathcal{D}\varphi, \psi, \mathcal{D}\psi)$. For sake of better readability, from now on we drop the dependence of $A_i^{(\varepsilon)}$, $i = 1, 2$ and $j^{(\varepsilon)}$ on the space variable x. In what follows we compute the terms $\mathfrak{R}_1(u_0, p_0)$, $\mathfrak{R}_2(u_0, p_0)$ and $\partial_\ell \mathfrak{L}(0, u_0, p_0)$ of Proposition 1 for the Lagrangian $\mathfrak{L}$ separately as follows. For this purpose we first introduce the following abbreviations:

$$a_1(\varepsilon, \varphi, \psi) := \langle A_1^{(\varepsilon)}(\varphi, \mathcal{D}\varphi), \psi \rangle, a_2(\varepsilon, \varphi, \psi) := \langle A_2^{(\varepsilon)}(\varphi, \mathcal{D}\varphi), \mathcal{D}\psi \rangle,$$

$$f_1(\varepsilon, \psi) := \langle F_1^{(\varepsilon)}, \psi \rangle, \qquad f_2(\varepsilon, \psi) := \langle F_2^{(\varepsilon)}, \mathcal{D}\psi \rangle,$$

$$J_1(\varepsilon, \psi) := J^{\mathrm{vol}}(\Omega_\varepsilon, \psi, \mathcal{D}\psi), \qquad J_2(\psi) := J^{\mathrm{bnd}}(\psi, \mathcal{D}\psi).$$

Then we split for instance $\mathfrak{R}_1(u_0, p_0)$ into the parts coming from $a_1, a_2, f_1, f_2, J_1, J_2$. The term coming from a_1 contributing to $\mathfrak{R}_1(u_0, p_0)$ is for instance given by

$$\mathfrak{R}_1^{A_1}(u_0, p_0) := \lim_{\varepsilon \searrow 0} \frac{1}{|\omega_\varepsilon|} \int_0^1 [\partial_\varphi a_1(\varepsilon, u_0 + s(u_\varepsilon - u_0), p_0) - \partial_\varphi a_1(\varepsilon, u_0, p_0)] \, (u_\varepsilon - u_0) \, ds, \quad (2.18)$$

where $\partial_\varphi a_1$ denotes the derivative with respect to the second argument. Similarly we denote by $\mathfrak{R}_1^{A_2}(u_0, p_0)$ and $\mathfrak{R}_1^{J_1}(u_0, p_0)$ the contributions of a_2 and J_1 to the term $\mathfrak{R}_1(u_0, p_0)$, respectively. We proceed in the same fashion for each term. The detailed computations are outlined in the following subsections. Additionally to Assumption 1 we make the following assumption.

Assumption 2. *We assume that p_0 is continuously differentiable at z.*

2.5.1. *Terms coming from $A_1^{(\varepsilon)}$.* For $A_1^{(\varepsilon)} : \mathbf{R}^m \times \mathbf{R}^{m \times d} \to \mathbf{R}^m$ let $\partial_{y_1} A_1^{(\varepsilon)} : \mathbf{R}^m \times \mathbf{R}^{m \times d} \to \mathcal{L}(\mathbf{R}^m, \mathbf{R}^m)$ denote the derivative with respect to the first argument and $\partial_{y_2} A_1^{(\varepsilon)} : \mathbf{R}^m \times \mathbf{R}^{m \times d} \to \mathcal{L}(\mathbf{R}^{m \times d}, \mathbf{R}^m)$ the derivative with respect to the second argument. We compute

$$\mathfrak{R}_{1,\varepsilon}^{A_1} := \int_0^1 [\partial_\varphi a_1(\varepsilon, u_0 + s(u_\varepsilon - u_0), p_0) - \partial_\varphi a_1(\varepsilon, u_0, p_0)] \, (u_\varepsilon - u_0) \, ds$$

$$= \int_0^1 \int_{\mathsf{D}} [\partial_{y_1} A_1^{(\varepsilon)}(u_0 + s(u_\varepsilon - u_0), \mathcal{D}u_0 + s\mathcal{D}(u_\varepsilon - u_0)) - \partial_{y_1} A_1^{(\varepsilon)}(u_0, \mathcal{D}u_0)](u_\varepsilon - u_0) \cdot p_0 \, dx \, ds$$

$$+ \int_0^1 \int_{\mathsf{D}} [\partial_{y_2} A_1^{(\varepsilon)}(u_0 + s(u_\varepsilon - u_0), \mathcal{D}u_0 + s\mathcal{D}(u_\varepsilon - u_0))$$

$$- \partial_{y_2} A_1^{(\varepsilon)}(u_0, \mathcal{D}u_0)](\mathcal{D}(u_\varepsilon - u_0)) \cdot p_0 \, dx \, ds.$$

Thus changing variables and using $(\mathcal{D}\varphi) \circ T_\varepsilon = \frac{1}{\varepsilon}\mathcal{D}(\varphi \circ T_\varepsilon)$ and $K_\varepsilon := \frac{(u_\varepsilon - u_0)\circ T_\varepsilon}{\varepsilon}$ yields

$$
\begin{aligned}
\mathfrak{R}_{1,\varepsilon}^{A_1} =\varepsilon^d \int_0^1 \int_{\mathsf{D}_\varepsilon} [\partial_{y_1} A_1^\omega(u_0 \circ T_\varepsilon + s\varepsilon K_\varepsilon, (\mathcal{D}u_0) \circ T_\varepsilon + s\mathcal{D}K_\varepsilon) \\
- \partial_{y_1} A_1^\omega(u_0 \circ T_\varepsilon, (\mathcal{D}u_0)\circ T_\varepsilon)](\varepsilon K_\varepsilon) \cdot (p_0 \circ T_\varepsilon)\, dx\, ds \\
+ \varepsilon^d \int_0^1 \int_{\mathsf{D}_\varepsilon} [\partial_{y_2} A_1^\omega(u_0 \circ T_\varepsilon + s\varepsilon K_\varepsilon, (\mathcal{D}u_0) \circ T_\varepsilon + s\mathcal{D}K_\varepsilon) \\
- \partial_{y_2} A_1^\omega(u_0 \circ T_\varepsilon, (\mathcal{D}u_0)\circ T_\varepsilon)](\mathcal{D}K_\varepsilon) \cdot (p_0 \circ T_\varepsilon)\, dx\, ds.
\end{aligned}
$$

Therefore setting $\mathfrak{R}_1^{A_1}(u_0, p_0) = \lim_{\varepsilon \searrow 0}\frac{1}{|\omega_\varepsilon|}\mathfrak{R}_{1,\varepsilon}^{A_1}$, we obtain

$$
\begin{aligned}
\mathfrak{R}_1^{A_1}(u_0, p_0) = \frac{1}{|\omega|}\int_{\mathbf{R}^d} [A_1^\omega(u_0(z), \mathcal{D}u_0(z) + \mathcal{D}K) - A_1^\omega(u_0(z), \mathcal{D}u_0(z)) \\
- \partial_{y_2} A_1^\omega(u_0(z), \mathcal{D}u_0(z))(\mathcal{D}K)] \cdot p_0(z)\, dx.
\end{aligned}
$$

Next, we compute

$$
\begin{aligned}
\mathfrak{R}_{2,\varepsilon}^{A_1} &:= [\partial_\varphi a_1(\varepsilon, u_0, p_0) - \partial_\varphi a_1(0, u_0, p_0)]\,(u_\varepsilon - u_0) \\
&= \int_\mathsf{D} [\partial_{y_1} A_1^{(\varepsilon)}(u_0, \mathcal{D}u_0) - \partial_{y_1} A_1^{(0)}(u_0, \mathcal{D}u_0)](u_\varepsilon - u_0) \cdot p_0\, dx \\
&\quad + \int_\mathsf{D} [\partial_{y_2} A_1^{(\varepsilon)}(u_0, \mathcal{D}u_0) - \partial_{y_2} A_1^{(0)}(u_0, \mathcal{D}u_0)](\mathcal{D}(u_\varepsilon - u_0)) \cdot p_0\, dx.
\end{aligned}
$$

Thus changing variables and using $(\mathcal{D}\varphi) \circ T_\varepsilon = \frac{1}{\varepsilon}\mathcal{D}(\varphi \circ T_\varepsilon)$ and $K_\varepsilon := \frac{(u_\varepsilon - u_0)\circ T_\varepsilon}{\varepsilon}$ yields

$$
\begin{aligned}
\mathfrak{R}_{2,\varepsilon}^{A_1} =\varepsilon^d \int_\omega [\partial_{y_1} A_1^{\mathrm{in}}(u_0 \circ T_\varepsilon, (\mathcal{D}u_0)\circ T_\varepsilon) - \partial_{y_1} A_1^{\mathrm{out}}(u_0 \circ T_\varepsilon, (\mathcal{D}u_0)\circ T_\varepsilon)](\varepsilon K_\varepsilon) \cdot (p_0 \circ T_\varepsilon)\, dx \\
+ \varepsilon^d \int_\omega [\partial_{y_2} A_1^{\mathrm{in}}(u_0 \circ T_\varepsilon, (\mathcal{D}u_0)\circ T_\varepsilon) - \partial_{y_2} A_1^{\mathrm{out}}(u_0 \circ T_\varepsilon, (\mathcal{D}u_0)\circ T_\varepsilon)](\mathcal{D}K_\varepsilon) \cdot (p_0 \circ T_\varepsilon)\, dx.
\end{aligned}
$$

Therefore setting $\mathfrak{R}_2^{A_1}(u_0, p_0) = \lim_{\varepsilon \searrow 0}\frac{1}{|\omega_\varepsilon|}\mathfrak{R}_{1,\varepsilon}^{A_1}$, we obtain

$$
\mathfrak{R}_2^{A_1}(u_0, p_0) = \frac{1}{|\omega|}\int_\omega [\partial_{y_2} A_1^{\mathrm{in}}(u_0(z), \mathcal{D}u_0(z)) - \partial_{y_2} A_1^{\mathrm{out}}(u_0(z), \mathcal{D}u_0(z))](\mathcal{D}K) \cdot p_0(z)\, dx.
$$

Finally we compute the term contributing to $\partial_\ell \mathfrak{L}(0, u_0, p_0)$ coming from $A_1^{(\varepsilon)}$ by

$$
\partial_\ell \mathfrak{L}^{A_1}(0, u_0, p_0) = [A_1^{\mathrm{in}}(u_0(z), \mathcal{D}u_0(z)) - A_1^{\mathrm{out}}(u_0(z), \mathcal{D}u_0(z))] \cdot p_0(z).
$$

2.5.2. *Terms coming from $A_2^{(\varepsilon)}$.* For $A_2^{(\varepsilon)} : \mathbf{R}^m \times \mathbf{R}^{m\times d} \to \mathbf{R}^{m\times d}$ let $\partial_{y_1} A_2^{(\varepsilon)} : \mathbf{R}^m \times \mathbf{R}^{m\times d} \to \mathcal{L}(\mathbf{R}^m, \mathbf{R}^{m\times d})$ denote the derivative with respect to the first argument and $\partial_{y_2} A_2^{(\varepsilon)} : \mathbf{R}^m \times \mathbf{R}^{m\times d} \to \mathcal{L}(\mathbf{R}^{m\times d}, \mathbf{R}^{m\times d})$ the derivative with respect to the second argument. We have

$$
\begin{aligned}
\mathfrak{R}_{1,\varepsilon}^{A_2} &= \int_0^1 (\partial_\varphi a_2(\varepsilon, u_0 + s(u_\varepsilon - u_0), p_0) - \partial_\varphi a_2(\varepsilon, u_0, p_0))\,(u_\varepsilon - u_0)\, ds \\
&= \int_0^1 \int_\mathsf{D} [\partial_{y_1} A_2^{(\varepsilon)}(u_0 + s(u_\varepsilon - u_0), \mathcal{D}u_0 + s\mathcal{D}(u_\varepsilon - u_0)) \\
&\qquad\qquad\qquad\qquad - \partial_{y_1} A_2^{(\varepsilon)}(u_0, \mathcal{D}u_0)](u_\varepsilon - u_0) : \mathcal{D}p_0\, dx\, ds \\
&\quad + \int_0^1 \int_\mathsf{D} [\partial_{y_2} A_2^{(\varepsilon)}(u_0 + s(u_\varepsilon - u_0), \mathcal{D}u_0 + s\mathcal{D}(u_\varepsilon - u_0)) \\
&\qquad\qquad\qquad\qquad - \partial_{y_2} A_2^{(\varepsilon)}(u_0, \mathcal{D}u_0)](\mathcal{D}(u_\varepsilon - u_0)) : \mathcal{D}p_0\, dx\, ds.
\end{aligned}
$$

Letting $\mathfrak{R}_1^{A_2}(u_0, p_0) := \lim_{\varepsilon \searrow 0} \frac{1}{|\omega_\varepsilon|} \mathfrak{R}_{1,\varepsilon}^{A_2}$ and following the same steps as in the computation of $\mathfrak{R}_1^{A_1}(u_0, p_0)$ above leads to

$$\mathfrak{R}_1^{A_2}(u_0, p_0) = \frac{1}{|\omega|} \int_{\mathbf{R}^d} [A_2^\omega(u_0(z), \mathcal{D}u_0(z) + \mathcal{D}K) - A_2^\omega(u_0(z), \mathcal{D}u_0(z))$$
$$- \partial_{y_2} A_2^\omega(u_0(z), \mathcal{D}u_0(z))(\mathcal{D}K)] : \mathcal{D}p_0(z) \ dx.$$

We further have

$$\mathfrak{R}_{2,\varepsilon}^{A_2} := [\partial_\varphi a_2(\varepsilon, u_0) - \partial_\varphi a_2(0, u_0)](u_\varepsilon - u_0)$$
$$= \int_{\mathsf{D}} [\partial_{y_1} A_2^{(\varepsilon)}(u_0, \mathcal{D}u_0) - \partial_{y_1} A_2^{(0)}(u_0, \mathcal{D}u_0)](u_\varepsilon - u_0) : \mathcal{D}p_0 \ dx$$
$$+ \int_{\mathsf{D}} [\partial_{y_2} A_2^{(\varepsilon)}(u_0, \mathcal{D}u_0) - \partial_{y_2} A_2^{(0)}(u_0, \mathcal{D}u_0)](\mathcal{D}(u_\varepsilon - u_0)) : \mathcal{D}p_0 \ dx.$$

Letting $\mathfrak{R}_2^{A_2}(u_0, p_0) := \lim_{\varepsilon \searrow 0} \frac{1}{|\omega_\varepsilon|} \mathfrak{R}_{2,\varepsilon}^{A_2}$ and following the same steps as in the computation of $\mathfrak{R}_2^{A_1}(u_0, p_0)$ leads to

$$\mathfrak{R}_2^{A_2}(u_0, p_0) = \frac{1}{|\omega|} \int_\omega [\partial_{y_2} A_2^{\text{in}}(u_0(z), \mathcal{D}u_0(z)) - \partial_{y_2} A_2^{\text{out}}(u_0(z), \mathcal{D}u_0(z))](\mathcal{D}K) : \mathcal{D}p_0(z) \ dx.$$
$$\tag{2.19}$$

Finally, the part of $\partial_\ell \mathfrak{L}(0, u_0, p_0)$ coming from $A_2^{(\varepsilon)}$ reads

$$\partial_\ell \mathfrak{L}^{A_2}(0, u_0, p_0) = [A_2^{\text{in}}(u_0(z), \mathcal{D}u_0(z)) - A_2^{\text{out}}(u_0(z), \mathcal{D}u_0(z))] : \mathcal{D}p_0(z).$$

2.5.3. *Terms coming from right hand side.* Since the right hand side does not depend on the solution and therefore $\partial_u F = 0$, there is no contribution to $\mathfrak{R}_1$ and $\mathfrak{R}_2$. It only remains

$$\partial_\ell \mathfrak{L}^F(0, u_0, p_0) = -(F_1^{\text{in}} - F_1^{\text{out}}) \cdot p_0(z) - (F_2^{\text{in}} - F_2^{\text{out}}) : \mathcal{D}p_0(z). \tag{2.20}$$

2.5.4. *Terms coming from J^{vol}.* Let $j_{y_1}^{(\varepsilon)} : \mathbf{R}^m \times \mathbf{R}^{m \times d} \to \mathcal{L}(\mathbf{R}^m, \mathbf{R})$ denote the derivative of $j^{(\varepsilon)}$ with respect to the first argument and $j_{y_2}^{(\varepsilon)} : \mathbf{R}^m \times \mathbf{R}^{m \times d} \to \mathcal{L}(\mathbf{R}^{m \times d}, \mathbf{R})$ the derivative with respect to the second argument such that

$$\partial_u J^{\text{vol}}(\Omega_\varepsilon, u, \mathcal{D}u)(\hat{u}) = \int_{\mathsf{D}} j_{y_1}^{(\varepsilon)}(u, \mathcal{D}u)(\hat{u}) + j_{y_2}^{(\varepsilon)}(u, \mathcal{D}u)(\mathcal{D}\hat{u}) \ dx. \tag{2.21}$$

We have

$$\mathfrak{R}_{1,\varepsilon}^{J^{\text{vol}}} := \int_0^1 (\partial_u J_1(\varepsilon, u_0 + s(u_\varepsilon - u_0)) - \partial_u J_1(\varepsilon, u_0))(u_\varepsilon - u_0) \ ds$$
$$= \int_0^1 [\partial_u J^{\text{vol}}(\Omega_\varepsilon, u_0 + s(u_\varepsilon - u_0), \mathcal{D}u_0 + s\mathcal{D}(u_\varepsilon - u_0))$$
$$- \partial_u J^{\text{vol}}(\Omega_\varepsilon, u_0, \mathcal{D}u_0)](u_\varepsilon - u_0) \ ds$$
$$= \int_0^1 \left\{ \int_{\mathsf{D}} [j_{y_1}^{(\varepsilon)}(u_0 + s(u_\varepsilon - u_0), \mathcal{D}u_0 + s\mathcal{D}(u_\varepsilon - u_0)) - j_{y_1}^{(\varepsilon)}(u_0, \mathcal{D}u_0)](u_\varepsilon - u_0) \ dx \right.$$
$$\left. + \int_{\mathsf{D}} [j_{y_2}^{(\varepsilon)}(u_0 + s(u_\varepsilon - u_0), \mathcal{D}u_0 + s\mathcal{D}(u_\varepsilon - u_0)) - j_{y_2}^{(\varepsilon)}(u_0, \mathcal{D}u_0)](\mathcal{D}(u_\varepsilon - u_0)) \ dx \right\} \ ds.$$

Therefore changing variables and using $(\mathcal{D}\varphi) \circ T_\varepsilon = \frac{1}{\varepsilon}\mathcal{D}(\varphi \circ T_\varepsilon)$ and $K_\varepsilon := \frac{(u_\varepsilon - u_0) \circ T_\varepsilon}{\varepsilon}$ yields

$$
\begin{aligned}
\mathfrak{R}_{1,\varepsilon}^{J^{\mathrm{vol}}} = \varepsilon^d \int_0^1 &\left\{ \int_{\mathsf{D}_\varepsilon} [j_{y_1}^{(\varepsilon)}(u_0 \circ T_\varepsilon + s\varepsilon K_\varepsilon, (\mathcal{D}u_0) \circ T_\varepsilon + s\mathcal{D}K_\varepsilon) \right. \\
&\qquad\qquad - j_{y_1}^{(\varepsilon)}(u_0 \circ T_\varepsilon, (\mathcal{D}u_0) \circ T_\varepsilon)](\varepsilon K_\varepsilon)\, dx \\
&+ \varepsilon^d \int_{\mathsf{D}_\varepsilon} [j_{y_2}^{(\varepsilon)}(u_0 \circ T_\varepsilon + s\varepsilon K_\varepsilon, (\mathcal{D}u_0) \circ T_\varepsilon + s\mathcal{D}K_\varepsilon) \\
&\qquad\qquad \left. - j_{y_2}^{(\varepsilon)}(u_0 \circ T_\varepsilon, (\mathcal{D}u_0) \circ T_\varepsilon)](\mathcal{D}K_\varepsilon)\, dx \right\}\, ds.
\end{aligned}
$$

Letting $\mathfrak{R}_1^{J^{\mathrm{vol}}}(u_0, p_0) := \lim_{\varepsilon \searrow 0} \frac{1}{|\omega_\varepsilon|}\mathfrak{R}_{1,\varepsilon}^{J^{\mathrm{vol}}}$ and using $\varepsilon K_\varepsilon \to 0$ and $\mathcal{D}K_\varepsilon \to \mathcal{D}K$, we obtain

$$
\begin{aligned}
\mathfrak{R}_1^{J^{\mathrm{vol}}}(u_0, p_0) = \frac{1}{|\omega|} \int_{\mathbf{R}^d} &[j^\omega(u_0(z), \mathcal{D}u_0(z) + \mathcal{D}K) - j^\omega(u_0(z), \mathcal{D}u_0(z)) \\
&- j_{y_2}^\omega(u_0(z), \mathcal{D}u_0(z))(\mathcal{D}K)]\, dx.
\end{aligned}
$$

Here, $j^\omega(y_1, y_2) = \chi_\omega\, j^{\mathrm{in}}(y_1, y_2) + \chi_{\mathbf{R}^d \setminus \omega}\, j^{\mathrm{out}}(y_1, y_2)$.

We proceed with the contribution of J^{vol} to the term $\mathfrak{R}_2(u_0, p_0)$. For this we compute

$$
\begin{aligned}
\mathfrak{R}_{2,\varepsilon}^{J^{\mathrm{vol}}} &:= [\partial_u J_1(\varepsilon, u_0) - \partial_u J_1(0, u_0)](u_\varepsilon - u_0) \\
&= [\partial_u J^{\mathrm{vol}}(\varepsilon, u_0, \mathcal{D}u_0) - \partial_u J^{\mathrm{vol}}(0, u_0, \mathcal{D}u_0)](u_\varepsilon - u_0) \\
&= \int_{\mathsf{D}} (j_{y_1}^{(\varepsilon)}(u_0, \mathcal{D}u_0) - j_{y_1}^{(0)}(u_0, \mathcal{D}u_0))(u_\varepsilon - u_0) \\
&\quad + \int_{\mathsf{D}} (j_{y_2}^{(\varepsilon)}(u_0, \mathcal{D}u_0) - j_{y_2}^{(0)}(u_0, \mathcal{D}u_0))(\mathcal{D}(u_\varepsilon - u_0)).
\end{aligned}
$$

Therefore setting $\mathfrak{R}_2^{J^{\mathrm{vol}}}(u_0, p_0) := \lim_{\varepsilon \searrow 0} \frac{1}{|\omega_\varepsilon|}\mathfrak{R}_{2,\varepsilon}^{J^{\mathrm{vol}}}$, we obtain

$$
\begin{aligned}
\mathfrak{R}_2^{J^{\mathrm{vol}}}(u_0, p_0) &= \lim_{\varepsilon \searrow 0} \frac{1}{|\omega_\varepsilon|} [\partial_u J^{\mathrm{vol}}(\varepsilon, u_0, \mathcal{D}u_0) - \partial_u J^{\mathrm{vol}}(0, u_0, \mathcal{D}u_0)](u_\varepsilon - u_0) \\
&= \lim_{\varepsilon \searrow 0} \frac{1}{|\omega_\varepsilon|} \left[\int_{\mathsf{D}} (j_{y_1}^{(\varepsilon)}(u_0, \mathcal{D}u_0) - j_{y_1}^{(0)}(u_0, \mathcal{D}u_0))(u_\varepsilon - u_0) \right. \\
&\qquad\qquad \left. + (j_{y_2}^{(\varepsilon)}(u_0, \mathcal{D}u_0) - j_{y_2}^{(0)}(u_0, \mathcal{D}u_0))(\mathcal{D}(u_\varepsilon - u_0))\, dx \right] \\
&= \lim_{\varepsilon \searrow 0} \frac{1}{|\omega|} \left[\int_\omega [j_{y_1}^{(\varepsilon)}(u_0 \circ T_\varepsilon, (\mathcal{D}u_0) \circ T_\varepsilon) - j_{y_1}^{(0)}(u_0 \circ T_\varepsilon, (\mathcal{D}u_0) \circ T_\varepsilon)](\varepsilon K_\varepsilon) \right. \\
&\qquad\qquad \left. + [j_{y_2}^{(\varepsilon)}(u_0 \circ T_\varepsilon, (\mathcal{D}u_0) \circ T_\varepsilon) - j_{y_2}^{(0)}(u_0 \circ T_\varepsilon, (\mathcal{D}u_0) \circ T_\varepsilon)](\mathcal{D}K_\varepsilon)\, dx \right] \\
&= \frac{1}{|\omega|} \int_\omega [j_{y_2}^{\mathrm{in}}(u_0(z), \mathcal{D}u_0(z)) - j_{y_2}^{\mathrm{out}}(u_0(z), \mathcal{D}u_0(z))](\mathcal{D}K)\, dx.
\end{aligned}
$$

Finally, the term of J^{vol} contributing to $\partial_\ell \mathfrak{L}$ reads

$$
\partial_\ell \mathfrak{L}^{J^{\mathrm{vol}}}(0, u_0, p_0) = j^{\mathrm{in}}(u_0(z), \mathcal{D}u_0(z)) - j^{\mathrm{out}}(u_0(z), \mathcal{D}u_0(z)). \tag{2.22}
$$

2.5.5. *Terms coming from* J^{bnd}. There is no contribution from the term J^{bnd}, since the rescaled term $\partial \mathsf{D}_\varepsilon$ tends to "infinity" and is therefore not present.

2.5.6. *Summary.* In summary we showed that

$$\mathfrak{R}_1(u_0, p_0) = \mathfrak{R}_1^{A_1}(u_0, p_0) + \mathfrak{R}_1^{A_2}(u_0, p_0) + \mathfrak{R}_1^{J^{\mathrm{vol}}}(u_0, p_0),$$

$$\mathfrak{R}_2(u_0, p_0) = \mathfrak{R}_2^{A_1}(u_0, p_0) + \mathfrak{R}_2^{A_2}(u_0, p_0) + \mathfrak{R}_2^{J^{\mathrm{vol}}}(u_0, p_0),$$

$$\partial_\ell \mathfrak{L}(u_0, p_0) = \partial_\ell \mathfrak{L}^{A_1}(u_0, p_0) + \partial_\ell \mathfrak{L}^{A_2}(u_0, p_0) + \partial_\ell \mathfrak{L}^{F}(u_0, p_0) + \partial_\ell \mathfrak{L}^{J^{\mathrm{vol}}}(u_0, p_0).$$

Therefore we proved the following theorem under the assumption that formally $\nabla K_\varepsilon \to \nabla K$ in $\mathbf{E}(\mathbf{R}^d)$ and $\varepsilon K_\varepsilon \to 0$ and that u_0 is sufficiently smooth at z.

Theorem 1. *The first order topological expansion of $\mathcal{J}$ at Ω) in the points z reads*

$$d\mathcal{J}(\Omega, \omega)(z) = \mathfrak{R}_1(u_0, p_0) + \mathfrak{R}_2(u_0, p_0) + \partial_\ell \mathfrak{L}(0, u_0, p_0), \tag{2.23}$$

where

$$\mathfrak{R}_1(u_0, p_0) = \frac{1}{|\omega|} \int_{\mathbf{R}^d} [A_1^\omega(u_0(z), \mathcal{D}u_0(z) + \mathcal{D}K) - A_1^\omega(u_0(z), \mathcal{D}u_0(z))$$
$$- \partial_{y_2} A_1^\omega(u_0(z), \mathcal{D}u_0(z))(\mathcal{D}K)] \cdot p_0(z) \, dx$$
$$+ \frac{1}{|\omega|} \int_{\mathbf{R}^d} [A_2^\omega(u_0(z), \mathcal{D}u_0(z) + \mathcal{D}K) - A_2^\omega(u_0(z), \mathcal{D}u_0(z))$$
$$- \partial_{y_2} A_2^\omega(u_0(z), \mathcal{D}u_0(z))(\mathcal{D}K)] : \mathcal{D}p_0(z) \, dx$$
$$+ \frac{1}{|\omega|} \int_{\mathbf{R}^d} [j^\omega(u_0(z), \mathcal{D}u_0(z) + \mathcal{D}K(x)) - j^\omega(u_0(z), \mathcal{D}u_0(z))$$
$$- j_{y_2}^\omega(u_0(z), \mathcal{D}u_0(z))(\mathcal{D}K)] \, dx$$

$$\mathfrak{R}_2(u_0, p_0) = \frac{1}{|\omega|} \int_\omega [\partial_{y_2} A_1^{in}(u_0(z), \mathcal{D}u_0(z)) - \partial_{y_2} A_1^{out}(u_0(z), \mathcal{D}u_0(z))](\mathcal{D}K) \cdot p_0(z) \, dx$$
$$+ \frac{1}{|\omega|} \int_\omega [\partial_{y_2} A_2^{in}(u_0(z), \mathcal{D}u_0(z)) - \partial_{y_2} A_2^{out}(u_0(z), \mathcal{D}u_0(z))](\mathcal{D}K) : \mathcal{D}p_0(z) \, dx$$
$$+ \frac{1}{|\omega|} \int_\omega [j_{y_2}^{in}(u_0(z), \mathcal{D}u_0(z)) - j_{y_2}^{out}(u_0(z), \mathcal{D}u_0(z))](\mathcal{D}K) \, dx$$

and

$$\partial_\ell \mathfrak{L}(0, u_0, p_0) = [A_1^{in}(u_0(z), \mathcal{D}u_0(z)) - A_1^{out}(u_0(z), \mathcal{D}u_0(z))] \cdot p_0(z)$$
$$+ [A_2^{in}(u_0(z), \mathcal{D}u_0(z)) - A_2^{out}(u_0(z), \mathcal{D}u_0(z))] : \mathcal{D}p_0(z)$$
$$- (F_1^{in} - F_1^{out}) \cdot p_0(z) - (F_2^{in} - F_2^{out}) : \mathcal{D}p_0(z)$$
$$+ j^{in}(u_0(z), \mathcal{D}u_0(z)) - j^{out}(u_0(z), \mathcal{D}u_0(z)).$$

The function K solves

$$\int_{\mathbf{R}^d} [A_2^\omega(z, u_0(z), \mathcal{D}u_0(z) + \mathcal{D}K) - A_2^\omega(z, u_0(z), \mathcal{D}u_0(z))] : \mathcal{D}\psi \, dx$$
$$= \int_\omega (F_2^{in} - F_2^{out})(z) : \mathcal{D}\psi \, dx - \int_\omega [A_2^{in} - A_2^{out}](z, u_0(z), \mathcal{D}u_0(z)) : \mathcal{D}\psi \, dx \tag{2.24}$$

for all $\psi \in \mathbf{E}(\mathbf{R}^d)$.

3. NUMERICAL EXPERIMENTS

In this section, we consider several linear and nonlinear problems in two and three space dimensions for which we numerically compute the topological derivative by means of the procedure outlined in the previous section, see the generic formulas of Theorem 1. We solve all underlying PDEs by means of piecewise linear and globally continuous finite elements on triangular grids using the finite element software package `NGSolve` [21]. We compute an approximation of the corrector function K, which is defined as the solution of a PDE on the unbounded domain $\mathbf{R}^d$, by solving (2.24) on a large, but bounded domain $B_R := B(\mathbf{0}, R)$ with homogeneous Dirichlet

boundary conditions on ∂B_R. This procedure is motivated by the fact that the solution K often can be shown to exhibit a decay behaviour as $|x| \to \infty$. We will show that the numerically computed topological derivative matches the analytical formula well for the topological derivative in cases where this formula is known. Moreover, we perform numerical tests to verify the topological asymptotic expansion

$$\mathcal{J}(\Omega_\varepsilon) = \mathcal{J}(\Omega) + \varepsilon^d |\omega| d\mathcal{J}(\Omega)(z) + \mathcal{O}(\varepsilon^{d+1}), \tag{3.1}$$

or, in other words

$$\delta \mathcal{J} := |\mathcal{J}(\Omega_\varepsilon) - \mathcal{J}(\Omega) + \varepsilon^d |\omega| d\mathcal{J}(\Omega)(z)| = \mathcal{O}(\varepsilon^{d+1}). \tag{3.2}$$

We consider several different inclusion shapes in two and three space dimensions. In 2D, we consider

(1) $\omega = \omega_{2D}^{(1)} := B((0,0), 1)$ the unit disk in $\mathbf{R}^2$
(2) $\omega = \omega_{2D}^{(2)} := B((0.5, 0.5), 1)$ a shifted unit disk in $\mathbf{R}^2$
(3) $\omega = \omega_{2D}^{(3)} := Ell((0,0), \frac{3}{2}, \frac{2}{3})$ an axis-aligned ellipse centered at the origin with axes lengths $\frac{3}{2}$ and $\frac{2}{3}$,
(4) $\omega = \omega_{2D}^{(4)} := Ell((0.5, 0.5), \frac{3}{2}, \frac{2}{3})$ a shifted axis-aligned ellipse centered at the point $(0.5, 0.5)^\top$ with the same axes lengths $\frac{3}{2}$ and $\frac{2}{3}$,
(5) $\omega = \omega_{2D}^{(5)} :=$ an L-shaped domain of area π,

and in 3D the shapes

(1) $\omega = \omega_{3D}^{(1)} := B((0,0,0), 1)$ the unit ball in $\mathbf{R}^3$
(2) $\omega = \omega_{3D}^{(2)} := B((0.5, 0.5, 0.5), 1)$ a shifted unit ball in $\mathbf{R}^3$
(3) $\omega = \omega_{3D}^{(3)} := Ell((0,0,0), \frac{3}{2}, \frac{2}{3}, 1)$ an axis-aligned ellipsoid centered at the origin with axes lengths $\frac{3}{2}$, $\frac{2}{3}$ and 1,
(4) $\omega = \omega_{3D}^{(4)} := Ell((0.5, 0.5, 0.5), \frac{3}{2}, \frac{2}{3}, 1)$ a shifted axis-aligned ellipsoid centered at the point $(0.5, 0.5, 0.5)^\top$ with the same axes lengths $\frac{3}{2}$, $\frac{2}{3}$ and 1.

Note that $\omega_{2D}^{(1)}$, $\omega_{2D}^{(3)}$, $\omega_{3D}^{(1)}$ and $\omega_{3D}^{(3)}$ are symmetric with respect to the x_1-, the x_2- (and the x_3-)axes while the other shapes are not.

The finite element software `NGSolve` allows to define PDEs in weak form in a symbolic way and also supports automated differentiation of expressions, see [16] for applications of these capabilities in the context of shape derivatives. Our implementation is available from [15]. It consists of a main file, which is completely independent of the concrete topology optimization problem at hand, and four other files defining the geometry, the PDE, the cost function as well as some algorithmic parameters. The main file implements the topological derivative of a general problem of the form (2.8), i.e., it implements the solution of the state and adjoint equation, of the corresponding corrector equation (2.24) on the large domain B_R as well as the computation of the terms $\Re_1(u_0, p_0)$, $\Re_2(u_0, p_0)$ and $\partial_\ell \mathfrak{L}(0, u_0, p_0)$ as they are given in Section 2.5.6.

3.1. **Diffusion, convection, reaction.** Here, we consider the class of topology optimization problems with tracking-type cost functionals and a scalar diffusion-convection-reaction equation as a PDE constraint. Given the computational domain whose boundary is divided into the disjoint Dirichlet and Neumann boundaries, $\partial \mathsf{D} = \Gamma_D \cup \Gamma_N$, the PDE-constrained topology optimization problem is to find $u \in H_{\Gamma_D}^1(\mathsf{D}) := \{v \in H^1(\mathsf{D}) : v|_{\Gamma_D} = 0\}$ and $\Omega \in \mathcal{A}$ for some set of admissible shapes $\mathcal{A}$ as a solution to

$$\min_\Omega J(u, \Omega) := \int_\mathsf{D} \tilde{\alpha}_\Omega(x) |u - u_d|^2 + \tilde{\beta}_\Omega(x) |\nabla(u - u_d)|^2 \, \mathrm{d}x + \tilde{\gamma} \int_{\Gamma_N} |u - u_d|^2 \, \mathrm{d}s \tag{3.3}$$

such that

$$\int_{\mathsf{D}} \beta_\Omega(x, |\nabla u|) \nabla u \cdot \nabla \psi + (\mathbf{b}_\Omega(x) \cdot \nabla u)\psi + \alpha_\Omega(x, u)\psi \; \mathrm{d}x \tag{3.4}$$

$$= \int_{\mathsf{D}} f_\Omega(x)\psi + \mathbf{M}_\Omega(x) \cdot \nabla \psi \; \mathrm{d}x + \int_{\Gamma_N} g_N \cdot \psi \; \mathrm{d}S \tag{3.5}$$

for all $\psi \in H^1_{\Gamma_D}(\mathsf{D})$. Here, $c_\Omega(x) := \chi_\Omega(x)c_1 + \chi_{\mathsf{D}\setminus\Omega}(x)c_2$ for some given constants c_1, c_2 for $c \in \{\tilde{\alpha}, \tilde{\beta}, \mathbf{b}, f, \mathbf{M}\}$. The functions $\beta_\Omega(x, |\nabla u|)$ and $\alpha_\Omega(x, u)$ will be defined piecewise in the subsequent subsections.

This problem fits into the framework considered in Section 2 with the choices

$$\begin{aligned} j^\Omega(x, u, \nabla u) =& \tilde{\alpha}_\Omega(x)|u - u_d|^2 + \tilde{\beta}_\Omega(x)|\nabla(u - u_d)|^2, \\ j^{bnd}(x, u, \nabla u) =& \tilde{\gamma}|u - u_d|^2, \\ A_1^\Omega(x, u, \nabla u) =& (\mathbf{b}_\Omega(x) \cdot \nabla u) + \alpha_\Omega(x, u), \\ A_2^\Omega(x, u, \nabla u) =& \beta_\Omega(x, |\nabla u|)\nabla u \\ F_1^\Omega(x) =& f_\Omega(x), \\ F_2^\Omega(x) =& \mathbf{M}_\Omega(x). \end{aligned}$$

3.1.1. *Example 1: A linear diffusion-convection-reaction problem in 2D.* We begin with a simple two-dimensional, linear version of problem (3.3)–(3.5) where we set $u_d = 0$, $\tilde{\alpha}_1 = 1$, $\tilde{\alpha}_2 = 2$, $\tilde{\beta}_1 = \tilde{\beta}_2 = 0$, $\tilde{\gamma} = 0$, $\mathbf{b}_1 = (1, 0)^\top$, $\mathbf{b}_2 = (0, 1)^\top$, $f_1 = 1$, $f_2 = 2$, $\mathbf{M}_1 = \mathbf{M}_2 = (0, 0)^\top$, $g_N(x_1, x_2) = x_1 x_2$. Moreover, we choose the piecewise constant functions

$$\begin{aligned} \beta_\varepsilon(x, |\nabla u|) =& \chi_{\Omega_\varepsilon}(x)\beta_1 + \chi_{\mathsf{D}\setminus\Omega_\varepsilon}(x)\beta_2, \\ \alpha_\varepsilon(x, u) =& \chi_{\Omega_\varepsilon}(x)\alpha_1 + \chi_{\mathsf{D}\setminus\Omega_\varepsilon}(x)\alpha_2, \end{aligned}$$

with the values $\beta_1 = 1$, $\beta_2 = 2$, $\alpha_1 = 1$, $\alpha_2 = 2$, which thus do not depend on u or ∇u.

In this setting, it is well-known that, for a point $z \in \mathsf{D} \setminus \Omega$ and inclusion shape $\omega = B_1(0)$ the unit disk, the corrector term K is linear inside ω and satisfies

$$\nabla K|_\omega = -\frac{\beta_1 - \beta_2}{\beta_1 + \beta_2} \nabla u(z), \tag{3.6}$$

see e.g. [13]. Thus, it follows that

$$\mathfrak{R}_2^{A_2}(u, p) = \frac{1}{|\omega|} \int_\omega (\beta_1 - \beta_2)\nabla K \cdot \nabla p(z) \; dx = -(\beta_1 - \beta_2)\frac{\beta_1 - \beta_2}{\beta_1 + \beta_2} \nabla u(z) \cdot \nabla p(z) \tag{3.7}$$

which together with the term $\partial_\ell \mathfrak{L}^{A_2}(u, p) = (\beta_1 - \beta_2)\nabla u(z) \cdot \nabla p(z)$ sums up to

$$\mathfrak{R}_2^{A_2}(u, p) + \partial_\ell \mathfrak{L}^{A_2}(u, p) = 2\beta_2 \frac{\beta_1 - \beta_2}{\beta_1 + \beta_2} \nabla u(z) \cdot \nabla p(z). \tag{3.8}$$

Similarly, $\partial_\ell \mathfrak{L}^{A_1}(u, p) = (\mathbf{b}_1 - \mathbf{b}_2) \cdot \nabla u(z)\, p(z) + (\alpha_1 - \alpha_2)u(z)p(z)$ together with

$$\mathfrak{R}_2^{A_1}(u, p) = \frac{1}{|\omega|} \int_\omega (\mathbf{b}_1 - \mathbf{b}_2) \cdot \nabla K\, p(z) \; dx = -\frac{\beta_1 - \beta_2}{\beta_1 + \beta_2}(\mathbf{b}_1 - \mathbf{b}_2) \cdot \nabla u(z)\, p(z) \tag{3.9}$$

adds up to

$$\mathfrak{R}_2^{A_1}(u, p) + \partial_\ell \mathfrak{L}^{A_1}(u, p) = 2\frac{\beta_2}{\beta_1 + \beta_2}(\mathbf{b}_1 - \mathbf{b}_2) \cdot \nabla u(z)\, p(z) + (\alpha_1 - \alpha_2)u(z)p(z). \tag{3.10}$$

Moreover, we have $\mathfrak{R}_1(u_0, p_0) = 0$ since the PDE constraint is linear and the cost function does not depend on ∇u. Together with the remaining terms $\partial_\ell \mathfrak{L}^F$ and $\partial_\ell \mathfrak{L}^{J^{\mathrm{vol}}}$, the topological

(a)   (b)   (c)
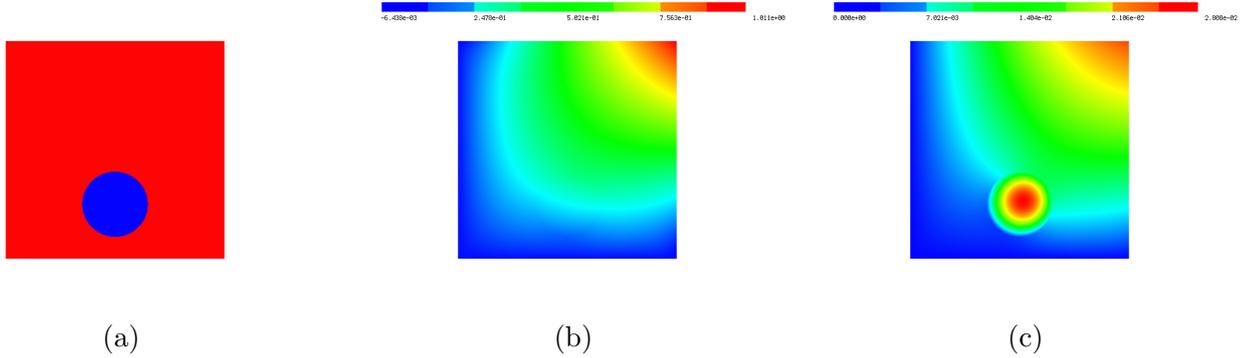
FIGURE 1. (a) Computational domain D with subdomain Ω for Examples 1 and 2. (b) Solution u to unperturbed state equation for linear Example 1. (c) Solution u to unperturbed state equation for nonlinear Example 2.

derivative reads in closed form,

$$
\begin{aligned}
d\mathcal{J}(\Omega,\omega)(z) =& 2\beta_2 \frac{\beta_1 - \beta_2}{\beta_1 + \beta_2}\nabla u(z) \cdot \nabla p(z) + 2\frac{\beta_2}{\beta_1 + \beta_2}(\mathbf{b}_1 - \mathbf{b}_2)\cdot \nabla u(z)\,p(z) + (\alpha_1 - \alpha_2)u(z)p(z) \\
& - (f_1 - f_2)p(z) + (\tilde{\alpha}_1 - \tilde{\alpha}_2)u(z)^2,
\end{aligned}
\tag{3.11}
$$

see also, e.g., [3] for the case where $\mathbf{b}_1 = \mathbf{b}_2 = (0,0)^\top$. A similar problem including a convection term is covered by the analysis in [7], however, there the factor $2\beta_2/(\beta_1 + \beta_2)$ (and thus the term $\mathfrak{R}_2^{A_1}(u,p)$) is missing. We remark that our numerical experiments indicate that this factor is important for having the correct topological derivative formula.

We numerically compute the topological derivative by the procedure explained in Section 2 for $\mathsf{D} = (-1,1)^2$ $\Gamma_D = \{(x_1, x_2) : x_1 = -1 \text{ or } x_2 = -1\}$, $\Gamma_N = \partial\mathsf{D} \setminus \Gamma_D$ and $\Omega = B((0,-0.5)^\top, 0.3)$ at the point $z = (0,0.5)^\top \in \mathsf{D} \setminus \Omega$ for the five inclusion shapes $\omega_{2D}^{(i)}$, $i = 1,\ldots,5$ defined above. Figure 1 depicts the computational domain D as well as the unperturbed state obtained on a mesh with 528724 vertices.

We solved the corresponding problem (2.24) for the corrector K on the bounded domain $B(\mathbf{0}, R)$ with $R = 1000$ using a finite element mesh consisting of 371950 vertices. In order to numerically verify the computed values, we performed a Taylor test for the topological asymptotic expansion (3.1). We chose a set of decreasing values for the inclusion radius ε, namely

$$
\underline{\varepsilon} := \{\varepsilon_0\,\delta^9, \ldots, \varepsilon_0\,\delta^1, \varepsilon_0\,\delta^0\}
\tag{3.12}
$$

with two constants $\varepsilon_0 = 0.005$ and $\delta = 1.5$, and solved the perturbed PDE constraint (2.9) on a mesh which is highly refined around the point z and evaluated the cost function to get perturbed cost function values $\mathcal{J}(\Omega_\varepsilon)$. For all $\varepsilon \in \underline{\varepsilon}$ and for each of the five inclusion shapes $\omega_{2D}^{(i)}$, we computed the quantities $\delta\mathcal{J}$ defined in (3.2). In Figure 2, it can be observed that, for each inclusion shape, $\delta\mathcal{J}$ behaves (at least) like ε^3. In the case of the two inclusions $\omega_{2D}^{(1)}$, $\omega_{2D}^{(3)}$ which are symmetric with respect to both the x_1- and the x_2-axes, we can even observe that $\delta\mathcal{J} = \mathcal{O}(\varepsilon^4)$. This is expected since it is known that the second term in the expansion (3.1) vanishes, $d^2\mathcal{J}(\Omega,\omega)(z) = 0$ for this example if symmetric inclusion shapes ω are considered, see e.g. [8]. In Figure 2 as well as in the subsequent Taylor test graphs, the data for $\omega_{2D}^{(i)}$, $i > 1$, is scaled such that they coincide with the data for $\omega_{2D}^{(1)}$ for the largest considered value of ε. This is done for better comparison of the convergence rates.

We will further investigate the numerically computed topological derivative for this example in Section 4 where we will also discuss the efficient evaluation of the topological derivative in the full computational domain D.
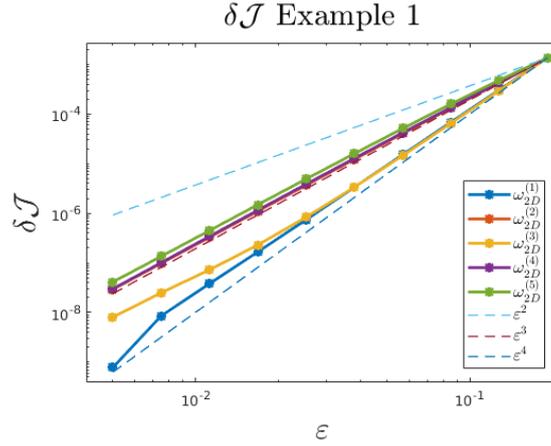
FIGURE 2. Numerical verification of topological asymptotic expansion (3.1) for Example 1 for five different inclusion shapes.
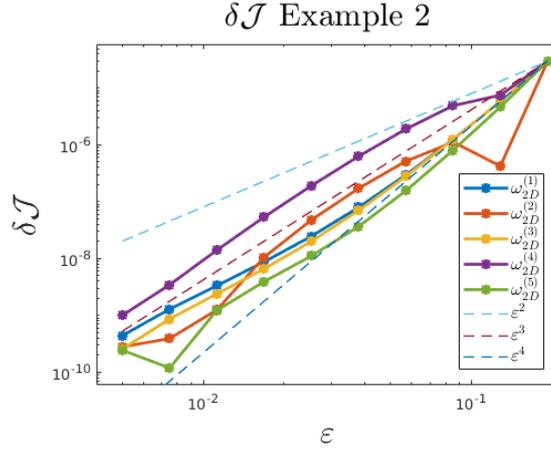
FIGURE 3. Numerical verification of topological asymptotic expansion (3.1) for Example 2 for five different inclusion shapes.

3.1.2. *Example 2: A nonlinear diffusion-convection-reaction problem in 2D.* Next, we consider a more general, quasilinear setting of problem (3.3)–(3.5) where we set $u_d = 0$, $\tilde{\alpha}_1 = 1$, $\tilde{\alpha}_2 = 2$, $\tilde{\beta}_1 = 1$, $\tilde{\beta}_2 = 2$, $\tilde{\gamma} = 1$, $\mathbf{b}_1 = (1,0)^\top$, $\mathbf{b}_2 = (0,1)^\top$, $f_1 = 1$, $f_2 = 2$, $\mathbf{M}_1 = (1,0)^\top$, $\mathbf{M}_2 = (0,1)^\top$, $g_N(x_1, x_2) = x_1 x_2$ as well as the nonlinear functions

$$\beta_\varepsilon(x, |\nabla u(x)|) = \begin{cases} 1 & x \in \Omega_\varepsilon, \\ \hat{\beta}_2(|\nabla u(x)|) & \text{else,} \end{cases} \qquad \alpha_\varepsilon(x, u(x)) = \begin{cases} 1 & x \in \Omega_\varepsilon, \\ u(x)^3 & \text{else,} \end{cases}$$

where $\hat{\beta}_2(s) = \nu_0 - (\nu_0 - 200)e^{-s^6/1000}$ with $\nu_0 = 10^7/(4\pi)$. This function is sometimes used as a magentic reluctivity function in electromagnetics and satisfies the monotonicity and Lipschitz conditions which ensure existence of a unique solution to the PDE constraint. Topological derivatives for problems involving quasilinear PDE constraints are challenging from both the analytical and the numerical point of view, see e.g. [5, 6, 12, 14]. The numerical experiments depicted in Figure 3 seem to exhibit the behavior $\mathcal{O}(\varepsilon^3)$ for all five inclusion shapes which is in accordance with (3.2) and therefore confirms the numerically computed value for the topological derivative.

3.1.3. *Example 3: A linear diffusion-convection-reaction problem in 3D.* Next, we consider a linear three-dimensional version of (3.3)–(3.5) on the domain $\mathsf{D} = B(\mathbf{0}, 1)$ with the subdomain
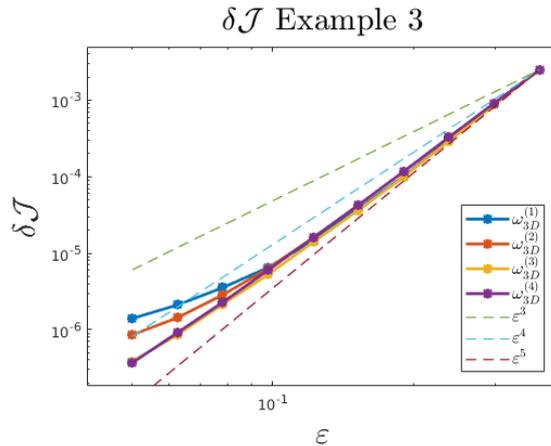
FIGURE 4. Numerical verification of topological asymptotic expansion (3.1) for Example 3 for four different inclusion shapes.
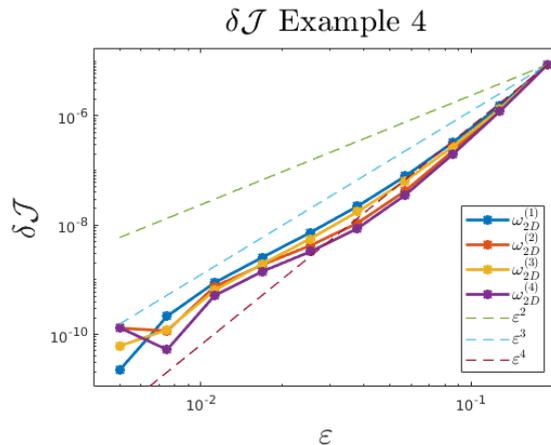
FIGURE 5. Numerical verification of topological asymptotic expansion (3.1) for Example 4 for four different inclusion shapes.

$\Omega = B((0, -0.7, 0)^\top, 0.2)$. We chose the parameters $u_d = 0$, $\tilde{\alpha}_1 = 1$, $\tilde{\alpha}_2 = 2$, $\tilde{\beta}_1 = \tilde{\beta}_2 = 0$, $\tilde{\gamma} = 0$, $\beta_1 = 1$, $\beta_2 = 2$, $\mathbf{b}_1 = \mathbf{b}_2 = (0, 0)^\top$, $f_1 = 1$, $f_2 = 2$, $\mathbf{M}_1 = \mathbf{M}_2 = (0, 0)^\top$, $g_N(x_1, x_2) = x_1 x_2$ and evaluate the topological derivative at the point $z = (0, 0.1, 0)^\top$. For each of the four inclusion shapes $\omega_{3D}^{(i)}$, $i = 1, 2, 3, 4$, we solved the corresponding corrector equation (2.24) on a three-dimensional ball B_R of radius $R = 1000$ using a tetrahedral mesh with 301116 vertices. Subsequently, we computed the topological derivative according to Section 2.5.6 and computed the quantities $\delta\mathcal{J}$ (3.2) for the vector of radius values (3.12) with $\varepsilon_0 = 0.05$ and $\delta = 1.25$. Figure 4 shows that the quantities $\delta\mathcal{J}$ decay at least as fast as ε^4 for all four inclusion shapes, which is in accordance with (3.1). The deterioration of the rates in Figure 4 can be attributed to the discretization error. We used a mesh consisting of 245177 vertices for the computational domain D which is highly refined around the point z.

3.2. **Elasticity.** In this section, we consider vector-valued partial differential equations coming from elasticity as PDE constraints. We consider the computational domain $\mathsf{D} = (0, 2) \times (0, 1)$ which is clamped at the top left and bottom left, $\Gamma_D = \{(x_1, x_2) : x_1 = 0 \text{ and } x_2 \in [0, 0.12] \cup [0.88, 1]\}$ and is subject to a downward directed force at $\Gamma_N = 1 \times (0.45, 0.55)$. On the rest of the boundary, $\Gamma := \partial\mathsf{D} \setminus (\Gamma_D \cup \Gamma_N)$, homogeneous Neumann boundary conditions are set. The domain consists of a strong material with Young's modulus $E = 1000$, and a very weak material which mimicks void inside $\Omega = B((0.5, 0.5)^\top, 0.3) \cup B((1.8, 0.25)^\top, 0.1) \cup B((1.8, 0.75)^\top, 0.1)$

(a)

(b)

(c)

(d)
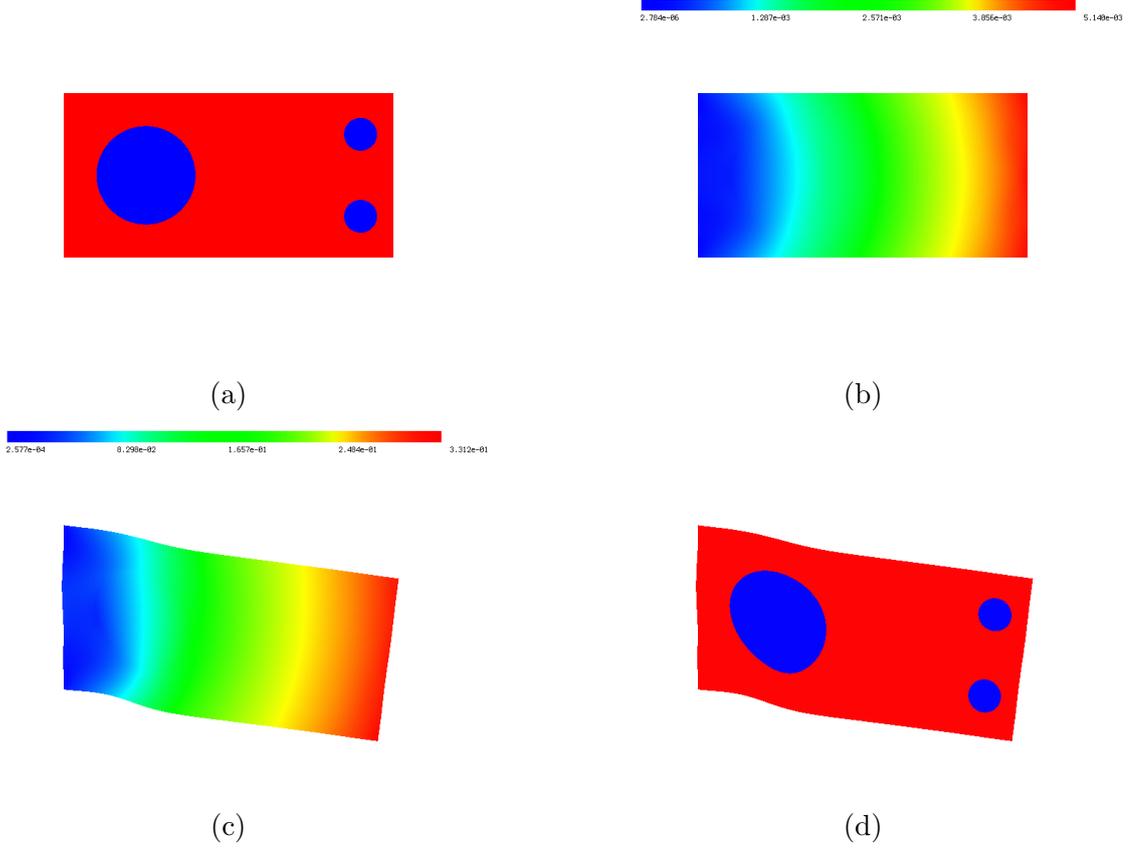
FIGURE 6. (a) Computational domain D with subdomain Ω for Examples 4 and 5. (b) Solution to linear state equation of Example 4 (undeformed). (c) Solution to nonlinear state equation of Example 5 in deformed configuration. (d) Deformed domain of Example 5.

where $E = 0.1$, see Figure 6(a). The Poisson ratio is set to $\nu = \frac{1}{3}$ in both subdomains. We consider the problem to minimize the compliance of the structure which is subject to self-weight as well as an external force acting on the boundary Γ_N. The problem reads

$$\min_{\Omega} \; J(u, \Omega) := \frac{1}{2} \int_{\mathsf{D}} S_{\Omega}(\mathcal{D}u) : \mathcal{D}u \; \mathrm{d}x \tag{3.13}$$

such that

$$u \in H^1_{\Gamma_D}(\mathsf{D})^d : \int_{\mathsf{D}} S_{\Omega}(\mathcal{D}u) : \mathcal{D}\psi \; \mathrm{d}x = \int_{\mathsf{D}} f_{\Omega} \cdot \psi \; \mathrm{d}x + \int_{\Gamma_N} g_N \cdot \psi \; \mathrm{d}S \tag{3.14}$$

for all $\psi \in H^1_{\Gamma_D}(\mathsf{D})^d$, where $S_{\Omega} : \mathbf{R}^{d \times d} \to \mathbf{R}^{d \times d}$ represents a stress tensor and f_{Ω} is a piecewise constant vector function. Also this problem fits into the framework considered in Section 2 by setting

$$
\begin{aligned}
j^{\Omega}(x, u(x), \mathcal{D}u(x)) =& \frac{1}{2} S_{\Omega}(\mathcal{D}u(x)) : \mathcal{D}u(x), \\
A^{\Omega}_1(x, u(x), \mathcal{D}u(x)) =& 0, \\
A^{\Omega}_2(x, u(x), \mathcal{D}u(x)) =& S_{\Omega}(\mathcal{D}u(x)), \\
F^{\Omega}_1(x) =& f_{\Omega}(x), \\
F^{\Omega}_2(x) =& 0.
\end{aligned}
$$

3.2.1. *Example 4: Linear elasticity in 2D.* We consider problem (3.13)–(3.14) for the two-dimensional cantilever example introduced above under a linear stress-strain relation,

$$S_\Omega(\mathcal{D}u) = 2\mu_\Omega e(u) + \lambda_\Omega Tr(e(u))I_2 \tag{3.15}$$

with the piecewise defined Lamé coefficients

$$\mu_\Omega(x) = \chi_\Omega(x)\mu_1 + \chi_{\mathsf{D}\setminus\Omega}(x)\mu_2, \qquad \lambda_\Omega(x) = \chi_\Omega(x)\lambda_1 + \chi_{\mathsf{D}\setminus\Omega}(x)\lambda_2,$$

corresponding to Young's modulus $E_2 = 1000$, $E_1 = 0.1$ and Poisson ratio $\nu_2 = \nu_1 = \frac{1}{3}$, i.e.,

$$\mu_i = E_i\frac{1}{2(1+\nu_i)} \qquad \lambda_i = E_i\frac{\nu_i}{(1+\nu_i)(1-2\nu_i)}, \quad \text{for } i = 1,2. \tag{3.16}$$

Here, $e(u) = \frac{1}{2}(\mathcal{D}u + \mathcal{D}u^\top)$ denotes the linearized strain tensor, $Tr(A)$ denotes the trace of a matrix A and I_2 denotes the two-dimensional identity matrix. Moreover, in this example we neglect self-weight, $f_\Omega = 0$, and consider the external load $g_N = (0,-1)^\top$ acting on Γ_N.

We computed the unperturbed state and adjoint on a mesh with about 150 000 vertices (resulting in about 300 000 degrees of freedom) which is highly refined around the point $z = (1.2, 0.5)^\top$ for which we compute and verify the topological derivative. We solve the corrector equation (2.24) with four considered two-dimensional inclusion shapes $\omega_{2D}^{(i)}$, $i = 1, \ldots 4$ where we replace the unbounded domain $\mathbf{R}^d$ by the large, but bounded domain $B_R = B(\mathbf{0}, R)$ with $R = 1000$ using a mesh with about 370 000 vertices. We again compute the quantities $\delta\mathcal{J}$ defined in (3.2) for a range of values for the inclusion radius ε (3.12) with $\varepsilon_0 = 0.005$ and $\delta = 1.5$. The behavior of $\delta\mathcal{J}$ for these five inclusion shapes can be seen in Figure 5 where we can again observe the behavior $\delta\mathcal{J} = \mathcal{O}(\varepsilon^3)$ for all five inclusion shapes.

3.2.2. *Example 5: Nonlinear elasticity in 2D.* Finally, we consider problem (3.13)–(3.14) with the nonlinear St. Venant-Kirchhoff material

$$S_\Omega(\mathcal{D}u) := (I_2 + \mathcal{D}u)\left[\lambda_\Omega \mathrm{Tr}(\frac{1}{2}(C(\mathcal{D}u) - I_2))I_2 + \mu_\Omega(C(\mathcal{D}u) - I_2)\right], \tag{3.17}$$

with $C(\mathcal{D}u) := (I_2 + \mathcal{D}u)^\top(I_2 + \mathcal{D}u) = I_2 + \mathcal{D}u + \mathcal{D}u^\top + \mathcal{D}u^\top\mathcal{D}u$, and $\lambda_\Omega = \chi_\Omega\lambda_1 + \chi_{\mathsf{D}\setminus\Omega}\lambda_2$, $\mu_\Omega = \chi_\Omega\mu_1 + \chi_{\mathsf{D}\setminus\Omega}\mu_2$ with $E_2 = 1000$, $E_1 = 0.1$ and $\nu_2 = \nu_1 = 0.3$ and $\lambda_1, \lambda_2, \mu_1, \mu_2$ defined as in (3.16). Here we use the larger external force $g_N = (0, -20)^\top$ acting on Γ_N and also mimic self-weight with $f_2 = (0, -5)^\top$, $f_1 = 0$.

For solving the state, adjoint and corrector equations, we use the same meshes as in Example 4. For solving the nonlinear state equation (2.4) we use a load stepping scheme with $N_{ls} = 20$ load steps where we gradually increase the loads given by f_2 and g_N until they reach their full values given above, i.e., we solve (2.4) with the data given above and

$$f_2 = \frac{k}{N_{ls}}\begin{pmatrix} 0 \\ -5 \end{pmatrix} \qquad g_N = \frac{k}{N_{ls}}\begin{pmatrix} 0 \\ -20 \end{pmatrix}$$

for $k = 1, \ldots N_{ls}$. For each load step, we use Newton's method to solve (2.4) for the given loads. The solution to the nonlinear state equation in deformed configuration can be seen in Figure 6(c) and the deformed domain in Figure 6(d). Moreover, we solve the corrector equation (2.24) by means of a damped Newton method with a very conservative damping factor of 0.002.

We performed a Taylor test by computing the quantities $\delta\mathcal{J}$ for the four inclusion shapes $\omega_{2D}^{(i)}$, $i = 1, 2, 3, 4$, using the same parameters $\underline{\varepsilon}$ as in Example 4. Figure 7 shows that $\delta\mathcal{J}$ decays at least as fast as ε^3 which confirms the topologcial asymptotic expansion (3.1).

4. On the efficient evaluation of topological derivatives in the full domain

In Section 3, we applied the systematic procedure for the computation of topological derivatives introduced in Section 2 to different model problems involving linear and nonlinear PDE constraints in two and three space dimensions. Moreover we verified the obtained values by Taylor tests. However, looking at the formulas of Section 2.5.6, it can be seen that the evaluation of the topological derivative at a spatial point z requires the solution of the corrector
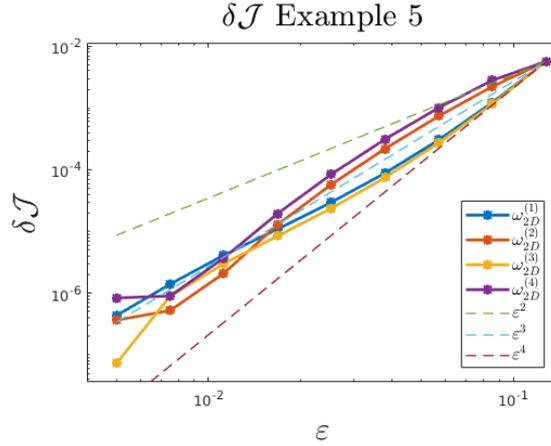
FIGURE 7. Numerical verification of topological asymptotic expansion (3.1) for Example 5 for four different inclusion shapes.

equation (2.24). On the other hand, in order to employ an optimization algorithm, one usually is interested in the topological derivative in the full design domain. Of course, solving (2.24) for every spatial point in the design domain (or every element of a mesh) is prohibitively expensive.

In the following, we show how, for linear or semilinear PDE constraints, the corresponding solution K can be obtained as a linear combination of some functions which can be precomputed. Note that, since we assume the PDE constraint to be linear or semilinear, both A_2^{in} and A_2^{out} are linear with respect to the third argument $\mathcal{D}u$ and constant with respect to the second argument u, i.e., there exist $a_2^{\text{in}}(z), a_2^{out}(z)$ such that

$$A_2^{\text{in}}(z, u_0(z), \mathcal{D}u_0(z)) = a_2^{\text{in}}(z)\mathcal{D}u_0(z) \quad \text{and} \quad A_2^{out}(z, u_0(z), \mathcal{D}u_0(z)) = a_2^{out}(z)\mathcal{D}u_0(z).$$

We introduce the notation

$$a_2^\omega(z, \mathcal{D}u_0(z)) := \chi_\omega(x)a_2^{\text{in}}(z)\mathcal{D}u_0(z) + \chi_{\mathbf{R}^d\setminus\omega}(x)a_2^{out}(z)\mathcal{D}u_0(z).$$

Now let $\hat{K}$ be the solution to

$$\int_{\mathbf{R}^d} a_2^\omega(z, \mathcal{D}\hat{K}) : \mathcal{D}\psi \, dx = \int_\omega (F_2^{\text{in}} - F_2^{out})(z) : \mathcal{D}\psi \, dx \tag{4.1}$$

for all ψ and, for $i \in \{1, \dots, m\}$, $j \in \{1, \dots, d\}$, let $\tilde{K}_{e_{ij}}$ be the solution to

$$\int_{\mathbf{R}^d} a_2^\omega(z, \mathcal{D}\tilde{K}_{e_{ij}}) : \mathcal{D}\psi \, dx = -\int_\omega (a_2^{\text{in}} - a_2^{out})(z)e_{ij} : \mathcal{D}\psi \, dx \tag{4.2}$$

for all ψ. Here $e_{ij} \in \mathbf{R}^{m\times d}$ denotes the unit basis element with the value 1 at the position (i, j) and the value 0 else.

These considerations immediately yield the following lemma.

Lemma 1. *Assume that the PDE constraint* (2.4) *is linear or semilinear and let* $\mathcal{D}u_0(z) \in \mathbf{R}^{m\times d}$ *be given. Then the solution* K *to* (2.24) *is given as the linear combination*

$$K = \hat{K} + \sum_{i=1}^m \sum_{j=1}^d (a_2^{in} - a_2^{out})(z)\mathcal{D}u_0(z)[i, j] \, \tilde{K}_{e_{ij}} \tag{4.3}$$

with $\hat{K}$ *and* $\tilde{K}_{e_{ij}}$ *given in* (4.1) *and* (4.2), *respectively.*

Using Lemma 1 it is possible to compute the solution K of (2.24) for any value of $\mathcal{D}u_0(z)$ by linear combination once the $md + 1$ functions $\hat{K}, \tilde{K}_{e_{ij}}$ have been computed. By integration over ω or $\mathbf{R}^d$ (which is numerically approximated by $B(\mathbf{0}, R)$ with $R = 1000$), the topological derivative can then be approximately evaluated at every point without having to solve an additional boundary value problem.
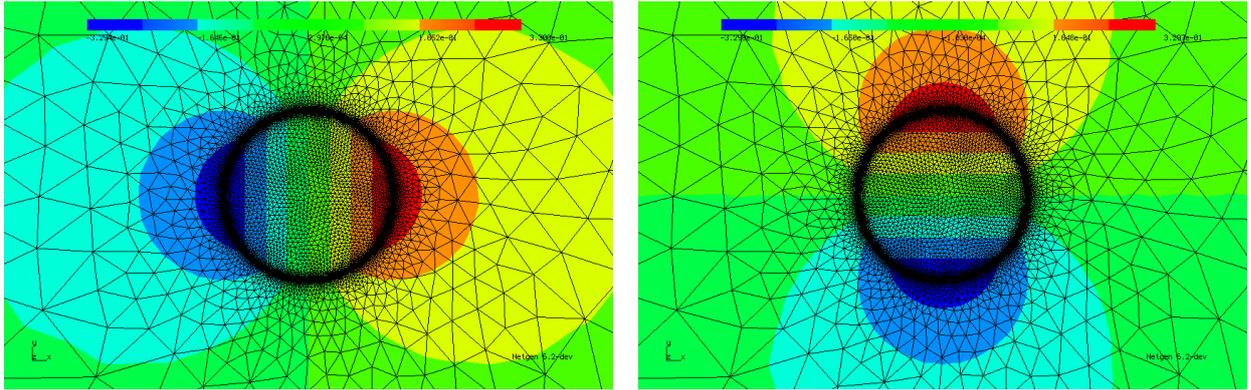
FIGURE 8. Solutions to (4.2) for $e_{11} = (1, 0)^{\top}$ (left) and $e_{12} = (0, 1)^{\top}$ (right).
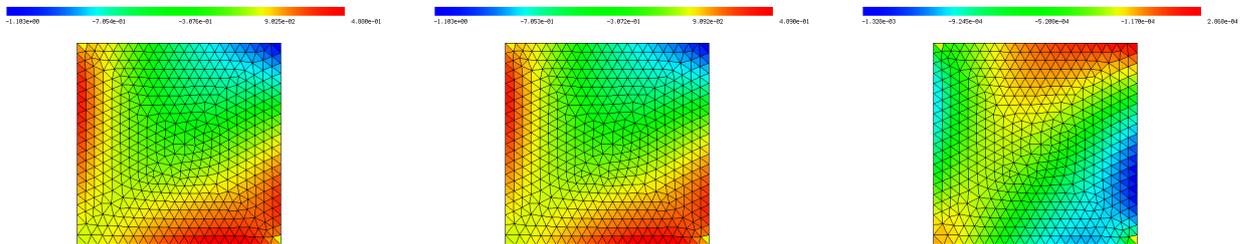
FIGURE 9. Left: Numerically computed topological derivative for Example 1. Center: Analytical formula (3.11). Right: Difference between numerical and analytical formulas. Observe the different orders of magnitude.

In the case of Example 1 (Section 3.1.1), it follows from $\mathbf{M}_1 = \mathbf{M}_2 = (0, 0)^{\top}$ that $\hat{K} = 0$. Since $m = 1$, $d = 2$, we need to precompute the solutions to (4.2) for the two unit vectors in $\mathbf{R}^2$ and can obtain the solution K to (2.24) by Lemma 1. The solutions $\tilde{K}_{e_{11}}$ and $\tilde{K}_{e_{12}}$ to (4.2) with $\mathbf{R}^d$ replaced by $B(\mathbf{0}, 1000)$ are depicted in Figure 8.

Next, we chose a (comparably coarse) mesh with only background material, i.e. $\Omega = \emptyset$, and numerically computed the topological derivative for the centroid of every triangular element by evaluating the formulas of Section 2.5.6. Also here, integrals over $\mathbf{R}^d$ were approximated by integrals over the large, but bounded ball $B(\mathbf{0}, 1000)$. A comparison of the obtained results with the analytical formula for the topological derivative given in (3.11) showed good accordance, see Figure 9.

Remark 4. *The procedure described in this section is still computationally expensive since it involves the numerical computation of several integrals over ω and $B(\mathbf{0}, 1000)$ for each topological derivative evaluation.*

We remark that in many cases it is possible to exploit the (affine) linearity of the topological derivative $d\mathcal{J}$ (2.23) with respect to the adjoint state as well as some rotational symmetry property of K with respect to $\mathcal{D}u_0(z)$ to directly precompute the topological derivative $d\mathcal{J}$ for some basis elements and to obtain the full topological derivative as a linear combination of these values. We remark that such a procedure – if applicable – can be computationally cheaper and allow for the use of the obtained formulas in iterative topology optimization algorithms, see e.g. [6, 14] for more details.

CONCLUSION AND OUTLOOK

We have illustrated a systematic way of computing topological derivatives for a large class of PDE-constrained topology optimization problems. Using automated differentiation in `NGSolve`,

it was possible to compute all potential terms of the topological derivative for an abstract problem class. We showed the effectivity of the method in several linear and nonlinear model problems and verified the topological derivative formulas by computing the values of the topological asymptotic expansion that should be satisfied by the topological derivative.

The presented work can be extended in several directions. On the one hand, we only considered problems posed in an H^1 setting. We remark that the same procedure is possible for any differential operator $\mathcal{D}$ that scales as $(\mathcal{D}\varphi) \circ T_\varepsilon = \frac{1}{\varepsilon}\mathcal{D}(\varphi \circ T_\varepsilon)$. In particular, this also includes the *curl* operator, thus also allowing to treat $H(curl)$ problems as they arise in electromagnetics [14]. Moreover, for some linear problems, the computational effort for solving the corrector equation (2.24) could be reduced by employing a boundary element method rather than a finite element method on an approximation of the unbounded domain. Finally, a further topic of future research is the numerical analysis of the topological derivative with respect to mesh sizes in the bounded domain D and in the blown-up domain B_R as well as with respect to the radius R of the large domain.

<div align="center">REFERENCES</div>

[1] G. Allaire and F. Jouve. Coupling the level set method and the topological gradient in structural optimization. In Springer, editor, *IUTAM Symposium on Topological Design Optimization of Structures, Machines and Materials*, pages 3–12, 2006.

[2] H. Ammari and H. Kang. *Polarization and Moment Tensors*. Springer-Verlag New York, 2007.

[3] S. Amstutz. Sensitivity analysis with respect to a local perturbation of the material property. *Asymptotic analysis*, 49(1), 2006.

[4] S. Amstutz and H. Andrä. A new algorithm for topology optimization using a level-set method. *Journal of Computational Physics*, 216(2):573–588, 2006.

[5] S. Amstutz and A. Bonnafé. Topological derivatives for a class of quasilinear elliptic equations. *Journal de Mathématiques Pures et Appliquées*, 107(4):367–408, 2017.

[6] S. Amstutz and P. Gangl. Topological derivative for the nonlinear magnetostatic problem. *Electron. Trans. Numer. Anal.*, 51:169–218, 2019.

[7] S. Amstutz, A.A. Novotny, and N. Van Goethem. Topological sensitivity analysis for elliptic differential operators of order 2m. *Journal of Differential Equations*, 256(4):1735–1770, 2014.

[8] P. Baumann and K. Sturm. Adjoint based methods for the computation of higher order topological derivatives with an application to linear elasticity. *arXiv*, 2021.

[9] M. Burger, B. Hackl, and W. Ring. Incorporating topological derivatives into level set methods. *Journal of Computational Physics*, 194(1):344–362, 2004.

[10] M.C. Delfour. Control, shape, and topological derivatives via minimax differentiability of lagrangians. In *Springer INdAM Series*, pages 137–164. Springer International Publishing, 2018.

[11] H. A. Eschenauer, V. V. Kobelev, and A. Schumacher. Bubble method for topology and shape optimization of structures. *Structural optimization*, 8(1):42–51, 1994.

[12] P. Gangl and K. Sturm. A simplified derivation technique of topological derivatives for quasi-linear transmission problems. *ESAIM Control Optim. Calc. Var.*, 26:Paper No. 106, 20, 2020.

[13] P. Gangl and K. Sturm. Topological derivative for PDEs on surfaces, 2020.

[14] P. Gangl and K. Sturm. Asymptotic analysis and topological derivative for 3d quasi-linear magnetostatics. *ESAIM: Mathematical Modelling and Numerical Analysis*, 55:S853–S875, 2021.

[15] P. Gangl and K. Sturm. Supplementary code for article "Automated computation of topological derivatives with application to nonlinear elasticity and reaction-diffusion problems", 2021. https://doi.org/10.5281/zenodo.5118379.

[16] P. Gangl, K. Sturm, M. Neunteufel, and J. Schöberl. Fully and semi-automated shape differentiation in NGSolve. *Structural and Multidisciplinary Optimization*, 63(3):1579–1607, November 2020.

[17] S. Garreau, P. Guillaume, and M. Masmoudi. The Topological Asymptotic for PDE Systems: The Elasticity Case. *SIAM Journal on Control and Optimization*, 39(6):1756–1778, 2001.

[18] M. Hintermüller. Fast level set based algorithms using shape and topological sensitivity information. *Control and Cybernetics*, 34(1), 2005.

[19] M. Hintermüller, A. Laurain, and A. A. Novotny. Second-order topological expansion for electrical impedance tomography. *Advances in Computational Mathematics*, 36(2):235–265, 2012.

[20] A. A. Novotny and J. Sokołowski. *Topological derivatives in shape optimization*. Interaction of Mechanics and Mathematics. Springer, Heidelberg, 2013.

[21] J. Schöberl. C++11 implementation of finite elements in NGSolve. Technical Report 30, Institute for Analysis and Scientific Computing, Vienna University of Technology, 2014.

[22] J. Sokołowski and A. Zochowski. On the topological derivative in shape optimization. *SIAM Journal on Control and Optimization*, 37(4):1251–1272, 1999.

[23] K. Sturm. Topological sensitivities via a Lagrangian approach for semilinear problems. *Nonlinearity*, 33(9):4310–4337, jul 2020.

(P. Gangl) TU GRAZ, STEYRERGASSE 30/III, 8010 GRAZ, AUSTRIA
Email address: gangl(at)math.tugraz.at

(K. Sturm) TU WIEN, WIEDNER HAUPTSTR. 8-10, 1040 VIENNA, AUSTRIA
Email address: kevin.sturm(at)tuwien.ac.at

Erschienene Preprints ab Nummer 2020/1

2020/1   D. Pacheco, T. Müller, O. Steinbach, G. Brenn: A mixed finite element formulation for generalised Newtonian fluid flows with appropriate natural outflow boundary conditions

2020/2   U. Langer, O. Steinbach, F. Tröltzsch, H. Yang: Unstructured space-time finite element methods for optimal sparse control of parabolic equations

2020/3   D.R.Q. Pacheco, R. Schussnig, O. Steinbach, T.-P. Fries: A fully consistent equal-order finite element method for incompressible flow problems

2020/4   U. Langer, O. Steinbach, F. Tröltzsch, H. Yang: Unstructured space-time finite element methods for optimal control of parabolic equations

2020/5   P. Gangl, K. Sturm, M. Neunteufel, J. Schöberl: Fully and Semi-Automated Shape Differentiation in NGSolve

2020/6   U. Langer, O. Steinbach, F. Tröltzsch, H. Yang: Space-time finite element discretization of parabolic optimal control problems with energy regularization

2020/7   G. Of, R. Watschinger: Complexity analysis of a fast directional matrix-vector multiplication

2020/8   P. Gangl, K. Sturm: Topological derivative for PDEs on surfaces

2020/9   D. R. Q. Pacheco, O. Steinbach: A continuous finite element framework for the pressure Poisson equation allowing non-Newtonian and compressible flow behaviour

2020/10 S. Kurz, S. Schöps, G. Unger, F. Wolf: Solving Maxwell's Eigenvalue Problem via Isogeometric Boundary Elements and a Contour Integral Method

2020/11 U. Langer, M. Schanz, O. Steinbach, W. L. Wendland (eds.): 18th Workshop on Fast Boundary Element Methods in Industrial Applications , Book of Abstracts

2020/12 P. Gangl, S. Köthe, C. Mellak, A. Cesarano, A. Mütze: Multi-objective free-form shape optimization of a synchronous reluctance machine

2021/1   O. Steinbach, M. Zank: A generalized inf-sup stable variational formulation for the wave equation

2021/2   U. Langer, O. Steinbach, H. Yang: Robust discretization and solvers for elliptic optimal control problems with energy regularization

2021/3   R. Löscher, O. Steinbach, M. Zank: Numerical results for an unconditionally stable space-time finite element method for the wave equation

2021/4   O. Steinbach, P. Gaulhofer: On space-time finite element domain decomposition methods for the heat equation

2021/5   D. R. Q. Pacheco, O. Steinbach: Space-time finite element tearing and interconnecting domain decomposition methods

2021/6   U. Langer, O. Steinbach, F. Tröltzsch, H. Yang: Space-time finite element methods for the initial temperature reconstruction

2021/7   J. Zapletal, R. Watschinger, G. Of, M. Merta: Semi-analytic integration for a parallel space-time boundary element method modeling the heat equation

2021/8   R. Watschinger, G. Of: An integration by parts formula for the bilinear form of the hypersingular boundary integral operator for the transient heat equation in three spatial dimensions

2021/9   O. Steinbach, C. Urzua-Torres: A new approach to space-time boundary integral equations for the wave equation

2021/10 O. Steinbach, C. Urzua-Torres, M. Zank: Towards coercive boundary element methods for the wave equation

2021/11 R. Watschinger, M. Merta, G. Of, J. Zapletal: A parallel fast multipole method for a space-time boundary element method for the heat equation

2021/12 T. Gauthey, P. Gangl, M. Hage Hassan: Multi-Material Topology Optimization with Continuous Magnetization Direction for Permanent Magnet Synchronous Reluctance Motors